PAPERS PRESENTED TO THE

WORKSHOP ON THE EVOLUTION OF THE MARTIAN ATMOSPHERE

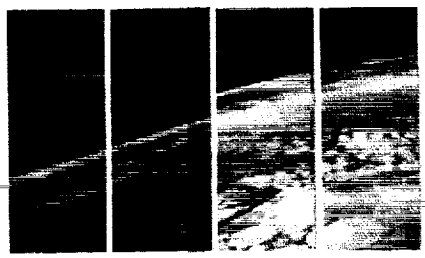

MSATT

Mars Surface and Atmosphere Through Time

Kona, Hawaii
June 29–July 1, 1992

Sponsored by

Lunar and Planetary Institute
The MSATT Study Group

PAPERS PRESENTED TO THE

WORKSHOP ON THE EVOLUTION OF THE MARTIAN ATMOSPHERE

Kona, Hawaii
June 29–July 1, 1992

Sponsored by
Lunar and Planetary Institute
The MSATT Study Group

LPI Contribution No. 787

Compiled in 1992 by

Lunar and Planetary Institute
3600 Bay Area Boulevard
Houston TX 77058-1113

The Lunar and Planetary Institute is operated by the Universities Space Research Association under Contract No. NASW-4574 with the National Aeronautics and Space Administration.

PREFACE

This volume contains papers that have been accepted for the Workshop on the Evolution of the Martian Atmosphere, June 29–July 1, 1992, in Kona, Hawaii. The Program Committee consisted of co-conveners Bruce Jakosky (University of Colorado, Boulder) and Janet Luhmann (University of California, Los Angeles).

Logistics and administrative support were provided by the Program Services Department staff at the Lunar and Planetary Institute. This volume was prepared by the Publications Services Department staff at the Lunar and Planetary Institute.

CONTENTS

Papers Presented to the Workshop on the Evolution of the Martian Atmosphere

N92-28479

The Impact of Temperature Dependent CO_2 Cross Section Measurements: A Role for Heterogeneous Chemistry in the Atmosphere of Mars?

A. D. Anbar, M. Allen, H. Nair, M-T. Leu, and Y. L. Yung, Division of Geological and Planetary Sciences 170–25, California Institute of Technology, Pasadena CA 91125, USA.

Carbon dioxide comprises over 95% of the atmosphere of Mars, despite continuous photolysis of CO_2 by solar UV radiation. Since the direct recombination of CO and O is spin-forbidden, the chemical stability of CO_2 in the Martian atmosphere is thought to be the result of a HO_x-catalyzed recombination scheme [1,2]. Thus, the rate of CO oxidation is sensitive to the abundance and altitude distribution of the HO_x species, OH, H and HO_2. Most Martian atmospheric models have assumed that HO_x abundances are governed purely by gas-phase chemistry [3,4]. However, it is well established that reactive HO_x radicals are adsorbed by a wide variety of surfaces. We have combined laboratory studies of H, OH, and HO_2 adsorption on inorganic surfaces, observational data of aerosol distributions, and an updated photochemical model to demonstrate that adsorption on either dust or ice aerosols is capable of reducing HO_x abundances significantly, thereby retarding the rate of CO oxidation.

Such scavenging of HO_x species by aerosols may be necessary to balance CO_2 production and loss. The inclusion of temperature dependent CO_2 cross sections [5] in Martian atmospheric models lowers the rate of CO_2 photolysis, while increasing the supply of HO_x via photolysis of H_2O [6]. This appears to result in an excessively rapid rate of CO recombination when only pure gas-phase chemistry is considered [7]. This problem may be resolved either by invoking a globally averaged water vapor abundance 5-10 times lower than that observed by Viking [3], or by loss of HO_x via reactions on aerosol surfaces.

Previous discussions of the influence of heterogeneous chemistry on the Martian atmosphere have focussed on heterogeneous catalysis of CO oxidation [8,9,10], although surface catalyzed CO oxidation has not yet been observed under Martian atmospheric conditions. HO_x adsorption has typically been overlooked, although this phenomenon has been studied in the laboratory under conditions approaching those of the lower Martian atmosphere. Kong and McElroy [11] considered heterogeneous destruction of HO_x in their models, but only on the regolith at the Martian surface; reactions on aerosol surfaces (dust or ice) were not considered.

Our results indicate that the magnitude of HO_x depletion resulting from adsorption on aerosol surfaces may be comparable to that achieved by reduction of the water vapor abundance from ≈15 to 1.5 precipitable μm. The magnitude of HO_x depletion is sensitive to the adsorption coefficients and aerosol distributions included in the model. Further laboratory measurements of HO_x adsorption, as well as observational constraints on the seasonal variability of aerosol abundances and altitude distributions, are needed before firmer conclusions can be drawn.

References: [1] McElroy M. B. and Donahue T. M. (1972) *Science*, 986–988. [2] Parkinson T. M. and Hunten D. M. (1972) *J. Atmos. Sci.*, 1380–1390. [3] Shimazaki T. (1989) *J. Geomag. Geoelectr.*, 273–301. [4] Yung Y. L. et al. (1988) *Icarus*, 146–159. [5] Lewis B. R. and Carver J. H. (1983) *J. Quant. Spectrosc. Radiat. Transf.*, 297–309. [6] Anbar A. D. and Allen M. (1992) *J. Geophys. Res. Planets*, submitted. [7] Nair H. et al. (1992) in preparation. [8] Huguenin R. L et al. (1977) *Icarus*, 270–298. [9] Atreya S. K. and Blamont J. E. (1990) *Geophys. Res. Lett.*, 287–290. [10] Leu M.-T. et al. (1992) *J. Geophys. Res. Planets*, 2621–2627. [11] Kong T. Y. and McElroy M. B. (1977) *Icarus*, 168–189.

N92-28480

Surface vs. Atmospheric Origin of 2.1–2.5 μm Absorption Features in the Martian Spectrum.

James F. Bell III[1] and David Crisp[2], [1]Planetary Geosciences, University of Hawaii, Honolulu HI 96822, USA, [2]JPL/Caltech, Pasadena CA 91109, USA.

Background: For over twenty years the origin of subtle absorption features in the spectrum of Mars near 2.3 μm ("K" Band: 1.9–2.5 μm) has been debated. This spectral region contains gaseous absorption features predominantly from CO_2 and CO on Mars and from telluric H_2O and CO_2 [e.g., 1–3]. Other authors have also interpreted absorption features at these wavelengths as evidence for specific clay minerals [4,5] and bicarbonate minerals such as scapolite [6]. The discovery of both clays and/or bicarbonates on Mars would have important implications for the evolution of the martian atmosphere. Specifically, clay minerals constrain possible past climate histories and the degree to which the surface is currently in thermodynamic equilibrium with the atmosphere [7]. Bicarbonates (or bisulfates) would provide a sink for the much more massive early CO_2 atmosphere proposed by some investigators [e.g., 8].

We have obtained new higher spectral resolution telescopic K band spectra of 10 surface regions from the IRTF at Mauna Kea during the 1990 opposition. Our goals are to confirm the existence of broad features seen at lower spectral resolution and to determine whether these bands are caused by atmospheric gases, surface (or airborne dust) minerals, or a combination of both.

Instrumentation, Observations, and Data Reduction: We used the IRTF Cooled Grating Array Spectrometer (CGAS) with its "B" grating to observe Mars in K band at a spectral resolution $R = \lambda/\Delta\lambda = 1200–1500$. This resolution is up to a factor of 5 greater than that employed by Clark et al. [6] and is adequate to crudely resolve Mars (and telluric) atmospheric bands, although $R > 50{,}000$ is necessary to resolve individual rotational lines. Our data were obtained on 15 and 16 November 1990 UT at a phase angle of 10°, $L_s = 333°$ and under clear skies and low relative humidity (2–20%). Each spectrum represents the average of 34 independent measurements of Mars minus sky voltage. Flux calibration was performed relative to IR standard stars (η Tau, β Leo, α Peg) and the Hardorp star HD28099 was observed as a solar analog. We obtained data across all of K band by stepping CGAS through 7 grating positions and allowing for several pixels of overlap between intervals. This technique was successfully used for Venus night side observations also in 1990 [9]. We observed 10 Mars surface regions in the western hemisphere during the 2 nights. Table 1 gives the locations and other information

TABLE 1. 1990 IRTF CGAS Mars data: Observational and geometric parameters.

Spot	UT Date	Time	Lat.	Lon.	Rad.	*i*	*e*	A	h	Name
1	11/15	0900	+10	83	680	32	38	0.31	4.6	Candor
2	11/15	0915	–25	56	590	14	18	0.16	4.2	Erythraeum
3	11/15	1400	+12	109	825	36	20	0.29	6.8	E. Tharsis
4	11/15	1415	–30	149	640	23	32	0.19	3.2	Sirenum
5	11/15	1430	–35	103	660	38	35	0.18	6.8	Claritas
6	11/16	000	+10	44	600	33	21	0.24	0.8	Chryse
7	11/16	1025	–14	53	595	15	10	0.16	3.0	Aurorae
8	11/16	1045	–42	34	695	44	42	0.20	3.0	Argyre
9	11/16	1220	+44	93	820	54	50	0.28	0.4	Ceraunius
10	11/16	1240	+8	123	635	29	33	0.28	5.6	W. Tharsis

Key: Lat., Lon., and Rad. are the latitude, longitude of the spot center and the effective radius (in km) of the area measured; i = incidence angle; e= emission angle; A = Albedo (IRTM broadband Viking data); h = elevation (km).

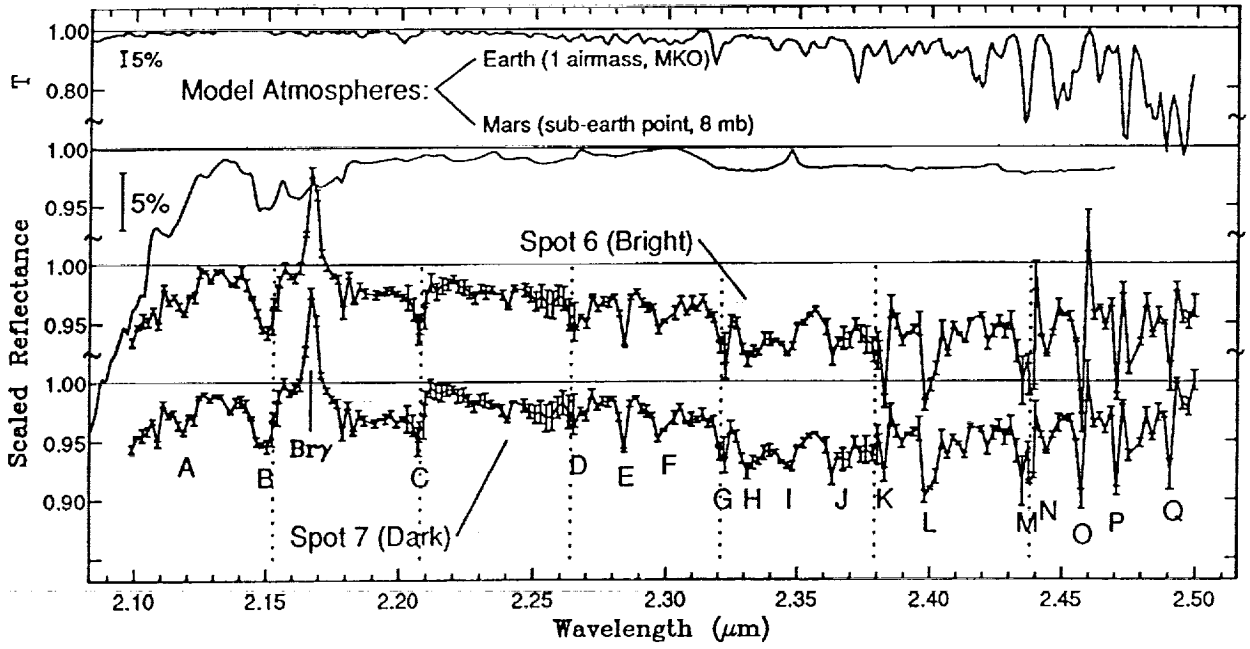

Fig. 1. 1990 CGAS Mars spectra compared to model terrestrial and martian atmospheres. Line labeled Brγ corresponds to the Brackett γ absorption feature in the IR standard star. Note scale change of telluric model.

about these 10 spots. We also obtained nearsimultaneous R = 100 whole-disk imaging spectroscopy across K band using the IRTF Proto CAM array camera [10]. These imaging spectroscopy data will be used to refine the absolute flux calibration and K band continuum slope of the CGAS spectra.

Preliminary Results and Interpretations: Figure 1 presents some of our preliminary results. This figure shows K band spectra of a bright and a dark region observed on 16 November 1990 UT. The Mars spectra have been divided by a 5770 K Planck function to yield the reflectance of Mars as a function of wavelength. Also plotted are a Mars model atmosphere [3] containing nominal dust abundance and at a surface pressure of 8 mb, and a telluric atmospheric transmission spectrum corresponding to 1.0 airmass at Mauna Kea Observatory. The Mars model spectrum has also had a 5770 K blackbody removed for comparison with the CGAS spectra. Wavelengths corresponding to the ends of each of the 7 spectral segments are indicated with dashed vertical lines.

There are many absorption features in these spectra, and there are only minor differences between the spectra of the bright and dark regions presented here. A list of the 17 absorption bands with a depth relative to the continuum ≥2.5% is contained in Table 2, along with preliminary band assignments. Both Mars and the standard star were observed under pristine sky conditions (clear, 2% RH) and within 0.02 airmass in order to remove contamination from telluric atmospheric gases. In spite of this, some of the most pronounced features in these spectra can be attributed to those gases (H_2O, CH_4, and N_2O). Other features (bands labeled E, K, and some of the broad 2.25–2.50 μm feature) may be related to CO in the solar spectrum. These solar and telluric contamination sources have not been fully considered previously, and could severely compromise the value of earlier lower spectral resolution Mars spectra. A notable exception to this is band L

2A.

TABLE 2. Band centers and preliminary assignments of most prominent features seen in spectra of Figure 1.

Band	(μm)	(cm^{-1})	Assignment
A	2.120	4717	Mars atm. CO_2^-
B	2.150	4651	Mars atm. CO_2
C	2.208	4529	⊕ CH_4?
D	2.267	4411	Mars atm. CO_2?
E	2.285	4376	Solar CO + ⊕ H_2O, N_2O
F	2.301	4346	⊕ N_2O + Mars Surface?
G	2.322	4307	⊕ CH_4, CO?
H	2.333	4286	⊕ CH_4 + Mars atm. CO?
I	2.347	4261	Mars atm. CO + ⊕ CH_4
J	2.367	4225	⊕CH_4 + Mars atm CO?
K	2.383	4196	⊕H_2O, CH_4 + Solar CO
L	2.400	4167	Mars surface + ?
M	2.437	4103	⊕ H_2O
N	2.445	4090	⊕ H_2O
O	2.458	4068	⊕ H_2O, N_2O?
P	2.471	4047	⊕ H_2O
Q	2.492	4013	⊕ H_2O

(2.396–2.404 μm), which we believe is a Mars surface absorption feature. The origin of this feature is unknown at this time.

Although these spectra appear "noisy" they accurately depict the martian K band spectrum, especially at $\lambda < 2.41$ μm where the telluric contamination is minimal. This conclusion is supported by (1) the small error bars and high S/N of the data (S/N = 300–1000); and (2) excellent agreement between the observations and the modeled Mars spectrum at several wavelengths such as near the 2.15 μm martian CO_2 band. Analyses of spectra of the 8 other regions observed and better-defined band assignments for the stronger and weaker features seen in the data will be presented at the conference.

References: [1] Connes J. P. et al. (1969) *CNES Special Line Atlas.* [2] Park J. H. et al. (1981) *NASA RP-1084.* [3] Crisp D. (1990) *JGR, 95,* 14577. [4] McCord T. B. et al. (1978) *JGR, 83,* 5433. [5] McCord T. B. et al. (1982) *JGR, 87,* 10129. [6] Clark R. N. et al. (1990) *JGR, 95,* 14463. [7] Gooding J. L. and Keil K. (1978) *CRL, 5,* 727. [8] Pollack J. B. et al. (1990) *JGR, 95,* 14595. [9] Bell J. F. III et al. (1991) *Science, 252,* 1293. [10] Bell J. F. III and Crisp D. (1991) *LPSC XXII,* 73–74.

N92-28481

A Photochemical Model for NH_3 in an Early Martian Atmosphere. L. L. Brown and J. F. Kasting, Department of Geosciences, Penn State University, University Park PA 16802, USA.

A warm and wet climate scenario for early Mars has been explained by invoking a 5-bar CO_2 atmosphere [1]; however, Kasting [2] has shown that CO_2 will condense in the Martian atmosphere at these pressures. The formation of CO_2 clouds will reduce the convective lapse rate and reduce the magnitude of the greenhouse effect. It is possible that additional greenhouse gases such as methane and ammonia were present in the early atmosphere of Mars. Ammonia was originally suggested as a greenhouse gas to compensate for reduced solar luminosity on the early Earth [3]. Kasting et al. [4] calculated that a surface temperature of 273 K could have been maintained on early Mars by a gas mixing ratio of $\sim 5 \times 10^{-4}$ by volume ammonia combined with a CO_2 partial pressure of 4–5 bars. Atmospheric ammonia is photochemically converted to N_2 by ultraviolet radiation at wavelengths shortward of 230 nm, therefore maintenance of sufficient ammonia concentrations would require a source of ammonia to balance the photolytic destruction.

We are using a one-dimensional photochemical model to estimate the magnitude of the ammonia source required to maintain a given ammonia concentration in a dense CO_2 atmosphere. For a surface temperature of 273 K, Kasting [2] predicts that condensation will occur at a CO_2 partial pressure greater than 1 bar. CO_2 clouds are nearly perfectly scattering at both solar and infrared wavelengths. At high CO_2 pressures, their contribution to the planetary albedo may dominate, producing a net cooling effect on surface temperatures. We will calculate photolysis rates for a range of ammonia concentrations, beginning with a CO_2 partial pressure of 1 bar.

Kasting [5] has calculated that ammonia in the Earth's early atmosphere would have been photochemically converted to N_2 at such a high rate as to prohibit sufficient accumulation for greenhouse warming. That calculation was performed for an atmosphere composed primarily of N_2. Because CO_2 is 2.5 times more efficient at Rayleigh scattering than N_2, we anticipate increased scattering opacities, and hence, decreased photolytic destruction rates of ammonia on early Mars. The reduced gravity on Mars means that a 1 bar atmosphere will be ~3 times as thick as a 1 bar atmosphere on Earth. This increased opacity will also reduce the destruction rate of ammonia in the Martian atmosphere. If ammonia were present in the early Martian atmosphere, it is probable that methane would be present as well. It is possible that ammonia could have been shielded from photolysis by hydrocarbon aerosols which form as a product of methane photolysis.

References: [1] Pollack J. B. et al. (1987) *Icarus, 71,* 203–224. [2] Kasting (1991) *Icarus, 94,* 1–13. [3] Sagan and Mullen (1972) *Science, 177,* 52–56. [4] Kasting et al. (1991) (abstract) In *Workshop on the Martian Surface and Atmosphere Through Time,* 71. [5] Kasting (1982) *J. Geophys. Res., 87,* 3091–3098.

N92-28482

Oxygen in the Martian Atmosphere: Regulation of P_{O2} by the Deposition of Iron Formations on Mars. Roger G. Burns, Department of Earth, Atmospheric and Planetary Sciences, Massachusetts Institute of Technology, Cambridge MA 02139, USA.

Introduction: During Earth's early history, and prior to the evolution of its present-day oxygenated atmosphere, extensive iron-rich siliceous sedimentary rocks were deposited [1,2], consisting of alternating layers of silica (chert) and iron oxide minerals (including hematite and magnetite). Such Precambrian banded iron-formations originated as submarine chemical precipitates of ferric oxides and chert when dissolved ferrous iron near the surface was oxidized by traces of oxygen in the Earth's

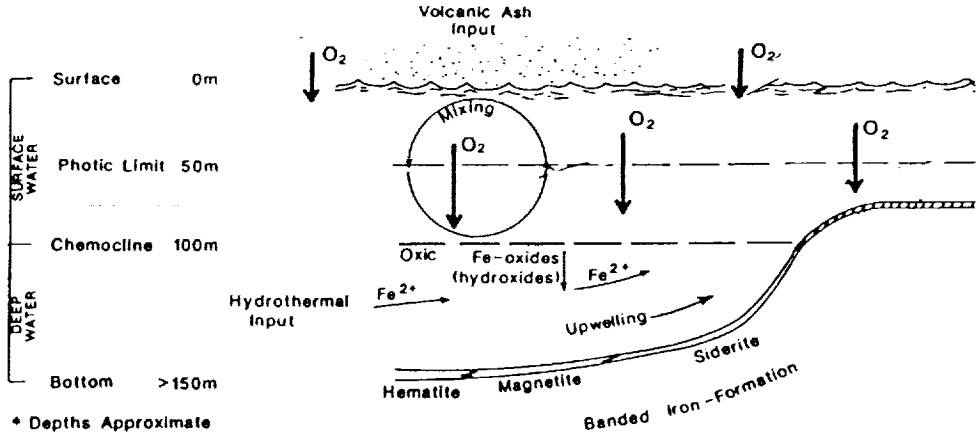

Fig. 1. Schematic depositional environment for the chemical precipitation of iron formations in a marine environment with a stratified water column (modified from ref. [6]).

early CO_2-dominated atmosphere [3–5]. The banding in iron formations recorded changes of atmosphere-hydrosphere interactions near sea level in the ancient ocean [6], which induced the oxidation of dissolved ferrous iron, precipitation of insoluble ferric oxides and silica, and regulation of oxygen in Earth's early atmosphere [5,7–9].

Similarities between the Archean Earth and the composition of the present-day atmosphere on Mars [10], together with the pervasive presence of ferric oxides in the martian regolith [11,12], suggested that iron formations might also have been deposited on Mars [13] and influenced the oxygen content of the martian atmosphere. Such a possibility is discussed here with a view to assessing whether the oxygen content of the martian atmosphere has been regulated by the chemical precipitation of iron formations on Mars.

Features of Banded Iron Formations: Deposition of terrestrial banded iron formations occurred during the Precambrian when oxygen levels in the atmosphere and, in particular, ocean depths were considerably lower than present-day values. Two major types of banded iron formations are recognized [1,2]: (1) the Lake Superior type, dominating the time period 2.5–2.0 b.y., which developed near shore on continental shelves under relatively stable tectonic conditions. Their deposition appears to have been influenced by oxygen produced by photosynthesis involving primitive life-forms in the palaeocean; (2) the Algoma type, dominating the 3.9–2.9 b.y. period in the Archean, which appear to be abiotic and associated with increased volcanism and high rates of mantle outgassing. Photochemical oxidation may have induced the deposition of these banded iron formations [14–17].

A third type of iron-formation, the Ratipan type (<1 b.y.), appears to be of glacial origin and to have formed when life was well established on Earth.

Thus, only inorganically produced Algonian-type banded iron formations would be applicable to Mars, assuming that biological activity has been absent on this planet.

Chemical Reactions Producing Banded Iron Formations: Three essential conditions had to exist in order for banded iron formations to be deposited. First, there had to be deep-water basins that were reducing, to account for the existence of sufficiently high steady-state concentrations of iron in solution. Second, surface waters had to be oxidizing, to induce the precipitation of ferric oxides. Third, upwelling was the transport mechanism between these reducting and oxidizing regimes. Thus, a stratified water column existed [18], consisting of a cold deep-water reservoir at a depth of several hundred meters, which was separated from the warmer aerated surface layer (50–100 m deep) by the chemocline where diffusion and advection occurred (Figure 1). Volcanogenic rocks (mafic lavas now greenstone belts) and exhalates provided the deep-water source of ferrous iron, much of which was leached from quenched glass, ferromagnesian silicate and sulphide minerals [19]. The Fe^{2+} ions derived from such dissolution processes could remain in solution indefinitely in near-neutral pH or acidic seawater [20,21], provided anoxic conditions existed at depth and dissolved sulfide anion levels were low [22]. High atmospheric CO_2 pressures would contribute to the acidity of the ocean [18]. Only when the increased supply of dissolved oxygen (by photosynthesis) outran the generation of dissolved iron did the oxidizing chemocline reach down into the deep reservoir, ultimately eliminating the source of mobile soluble iron.

Upwelling of Fe^{2+}-saturated water induced the oxidation of dissolved iron in the photic zone near the surface (Fig. 1), either by atmospheric oxygen (reaction {1}): $Fe^{2+}_{(aq)} + 1/4\ O_{2(aq)} + 3/2\ H_2O \rightarrow FeOOH_{(s)} + 2H^+_{(aq)}$ {1} derived from photolysis of water vapor and/or photosynthesis [18], or by photochemical oxidation of $FeOH^+$ complex ions [14–17] (reaction {2}): $Fe\ OH^+_{(aq)} + H_2O \xrightarrow{\text{uv light at 254 nm}} FeOOH_{(s)} + H_2O + 1/2\ H_{2\ (g)}$ {2}.

The kinetics of reaction {1} are so rapid at near-neutral pH [19–21], particularly in warm surface water, that oxidation of ferrous iron effectively removed dissolved oxygen from surface waters and maintained very low oxygen levels in the atmosphere of the Archean Earth. This situation existed while dissolved Fe^{2+} persisted in the deeper ocean and oxygen production at the surface was buffered by precipitation of ferric oxides. The rise of atmospheric oxygen on Earth due to photosynthesis eventually enabled oxygenated water to circulate deeper into the oceans, effectively removing dissolved ferrous iron, ceasing chemical precipitation of iron formations, and causing oxygen levels in the atmosphere to approach the present-day value ($P_{O2} = 10^{-0.68}$ bar).

Thus, Precambrian banded iron formations may have regulated the terrestrial atmospheric P_{O2} pressures between about 6×10^{-3} bar and 10^{-8} bar [7,8]. The question arises whether the present-day atmospheric P_{O2} on Mars ($P_{O2} = 10^{-5}$ bar) has also been influenced by the chemical precipitation of iron formations.

Chemical Modeling of Iron Formation Deposition: Evolutionary models for the Archean ocean-atmosphere system yielding chemical precipitation of banded iron formations have been computed [17,18]. In such models, the ocean was divided into three regions, a mixed surface layer at 20°C, the chemocline in which advection and diffusion of dissolved iron and atmospheric oxygen occurred, and a deep-water reservoir of soluble Fe at 5°C. The composition, salinity, and circulation rate of the ocean were assumed to be comparable to present-day seawater values. The influence of dissolved CO_2 on the pH of the ocean was determined for atmospheric CO_2 pressures ranging from 1 to 1000 times the present atmospheric level (PAL), which on Earth is currently about 3.5×10^{-4} bar. During the Archean, however, the P_{CO2} levels are believed to have been in the 100–1000 PAL range so as to maintain the surface temperature above the freezing point of water in the face of decreased luminosity [8,18]. Note that the present-day P_{CO2} of the martian atmosphere (6.3×10^{-3} bar) is about 20 times higher than that on Earth [10] and that higher atmospheric P_{CO2} levels have also been suggested for the early atmosphere of Mars [23]. Concentrations of dissolved Fe^{2+} ranging from 10^{-9} M to the saturation value determined by the solubility of siderite (approx. 10^{-4} M) were used to estimate the rate of oxidation of Fe^{2+} formulated by reaction {1}. Results are plotted in Fig. 2 for different atmospheric P_{CO2} levels.

Although four Fe^{2+} ions are oxidized per molecule of O_2 (reaction {1}), the rate of consumption of dissolved oxygen in the mixed surface layer would be sufficiently high to deplete oxygen in the atmosphere to about $P_{O2} = 10^{-8}$ bar [7]. Provided there was a steady source of dissolved ferrous iron below the chemocline and ocean circulation was sufficiently rapid to upwell Fe^{2+} saturated seawater to the surface, chemical precipitation of banded iron formations continued on Earth until the atmospheric pressure of oxygen built up to about 6×10^{-3} bar [8], or even higher [9], as a result of photosynthesis and the availability of organic carbon at depth to maintain a reducing regime to stabilize ferrous iron. Once the deep oceans became oxygenated, deposition of banded iron formations terminated on Earth.

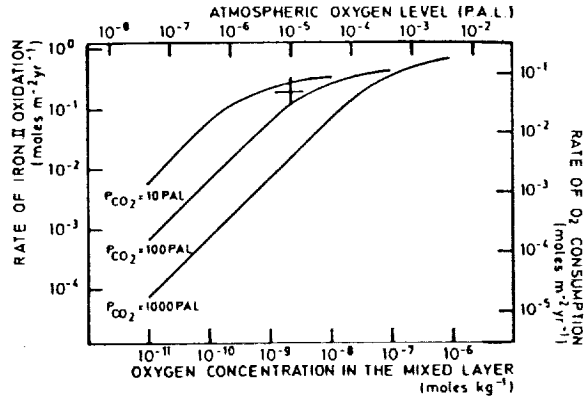

Fig. 2. Rate of oxidation of aqueous ferrous iron as a function of dissolved oxygen concentration in surface waters of a stratified ocean (based on ref. [18]). The concentration of Fe^{2+} corresponds to deep-water saturation by siderite. The equilibrium atmospheric P_{O2} is represented on the upper scale and the rate of consumption of O_2 is shown on the right-hand scale. + denotes the present-day atmospheric P_{CO2} and P_{O2} values for Mars.

Applications to Mars: The surface of Mars has many of the features required for the abiotic chemical precipitation of iron formations. First, ocean basins exceeding depths of about 1 km probably existed on lowland terrains on Mars. Second, iron-rich basaltic rocks erupting onto the martian surface were susceptible to chemical weathering in acidic environments believed to exist there, producing a copious supply of dissolved Fe^{2+} ions. Third, the dissolved ferrous iron was vulnerable to oxidation by dissolved oxygen formed by photolysis of water vapour in the atmosphere.

Reaction rates of oxidation of ferrous iron by dissolved oxygen shown in Fig. 2 were probably applicable to Mars when surface temperatures on that planet were higher in the past. According to Fig. 2, the present-day atmospheric P_{O2} on Mars (10^{-5} bar), together with the ratio: P_{CO2} (Mars)/P_{CO2} (Earth) which defines a PAL value of 20, indicate the rate of oxidation of aqueous Fe^{2+} to be about $10^{-0.6}$ M/sq.m/year and the rate of consumption of dissolved O_2 to be about $10^{-1.25}$ M/m^2/y. However, since the frozen regolith now prevents upwelling of Fe^{2+}-enriched subsurface aquifers, the present-day atmospheric P_{O2} may no longer be effectively regulated by the chemical precipitation of ferric oxides [24].

References: [1] Appel P. W. A. and LaBerge G. I., eds. (1987) *Precambrian Iron-Formations*, Theophrastus Publ. [2] James H. L. and Trendall A. F. (1982) In *Mineral Deposits and the Evolution of the Biosphere* (H. D. Holland and M. Schidlowski, eds.), pp. 201–217, Springer-Verlag. [3] Cloud P. (1973) *Econ. Geol., 68*, 1135–1143. [4] Drever J. I. (1974) *GSA Bull., 85*, 1099–1106. [5] Holland H. D. (1984) *The Chemical Evolution of the Atmosphere and Oceans*, Princeton Univ. [6] Klein C. and Beukes N. J. (1989) *Econ. Geol., 84*, 1733–1774. [7] Kasting J. F. and Walker J. C. G. (1981) *JGR, 86*, 1147–1158. [8] Kasting J. F. (1987) *Precamb. Res., 34*, 205–229. [9] Towe K. M. (1991) *Palaeogeog., Palaeoclim., Palaeoecol., 97*, 113–123. [10] Owen T. et al., *JGR, 82*, 4635–4640. [11] Singer R. B. (1985) *Adv. Space Res., 5*, 59–68. [12] Bell J. F. III et al. (1990) *JGR, 95*, 14447–14461. [13] Burns R. G. and Fisher D. S. (1990) *JGR, 95*, 14415–14421. [14] Cairns-Smith A. G. (1978) *Nature, 276*, 807–808. [15] Braterman P. S. et al. (1983) *Nature, 303*, 163–164. [16] Braterman P. S. and Cairns-Smith A. G. (1987) in ref. [1], pp. 215–242. [17] Francois L. M. (1986) *Nature, 320*, 352–354. [18] Francois L. M. and Gerard J-G. (1986) *Paleoceanography, 1*, 355–368. [19] Burns R. G. (1992) *LPS XXIII*, 187–188. [20] Burns R. G. (1992) *LPI Tech. Rpt. 92-02*, 26–27. [21] Sung W. and Morgan J. J. (1980) *Environ. Sci. Technol., 14*, 561–568. [22] Walker J. C. G. (1985) *Precamb. Res., 28*, 205–222. [23] Pollack J. B. et al. (1987) *Icarus, 71*, 203–224.
[24] Research supported by NASA grant no. NAGW-2220.

N92-28483

Water Inventories on Earth and Mars: Clues to Atmosphere Formation. M. H. Carr, U.S. Geological Survey, Menlo Park CA 94025, USA.

Water is distributed differently on Earth and Mars and the differences may have implications for the accretion of the two planets and formation of their atmospheres. The Earth has 2.7 km of water at or near the surface, most being in the oceans. The water content of the upper mantle appears to vary considerably from 150 ppm to several hundred ppm. The mantle as a whole is estimated to contain a few hundred ppm, but there is considerable uncertainty in this number because of uncertainty in the amounts of undepleted mantle and subducted crustal water that are present. Geologic evidence suggests that a few hundred meters of water are close to the martian surface. SNC meteorites are, however, very dry rocks. Assuming all the water evolved from SNCs at temperatures in excess of 400°C is martian, the martian mantle is estimated to contain about 40 ppm water. This estimate may be high, since oxygen isotopes suggest that some of the water in the SNCs may be from near-surface sources. Part of the difference in water content of the mantles of the two planets is clearly the result of plate tectonics. But the Earth's mantle appears to contain at least several times the water content of martian mantle, even accounting for plate tectonics. Two additional causes may have contributed to the different water content of the mantle of the two planets. The first possibility, suggested by the work of Matsui and Abe [1], is that the Earth's surface melted during accretion, as a result of development of a steam atmosphere, thereby allowing impact-devolatilized water at the surface to dissolve into the Earth's interior. In contrast, because of Mars' smaller size and greater distance from the Sun, the martian surface may not have melted, so that the devolatilized water could not dissolve into the surface. A second possibility is suggested by the pattern of siderophile elements in the Earth's mantle, which indicates that the Earth acquired a volatile-rich veneer after the core formed [2]. Mars does not have a comparable siderophile anomaly. Mars, like the Earth, may have acquired a late volatile-rich veneer, but it did not get folded into the interior as with the Earth, but instead remained as a water-rich veneer. The mantle was thus left dry and without the siderophile signature of the veneer. The perception of Mars as having a wet surface, but dry interior, is consistent with what we know of the geologic history of Mars, which can be viewed as the progressive intrusion and overplating of a water-rich crust by dry, mantle-derived volcanic rocks.

References: [1] Matsui T. and Abe Y. (1987) *Earth Moon and Planets, 39*, 207–214. [2] Wanke H. (1981) *Phil. Trans. R. Soc., London, A303*, 287–303.

N92-28484

Distribution of Martian Ground-Ice Table: Preliminary Results About Climatic Variations. F. M. Costard, Laboratoire de Geographie Physique, CNRS, 1 place Arsitide-Briand, 92195 Meudon Cedex, France.

Methodology: Rampart craters seem to have been emplaced by flows around craters over the surface just after the impact event by melting of volatiles [1,2]. Such rampart craters are considered to be good ground-ice indicators. In order to produce a valuable statistic of ground-ice table distribution, all rampart craters have been taken into account. Data were collected for 2600 rampart craters on all planet Mars in the size range 1–40 km [3].

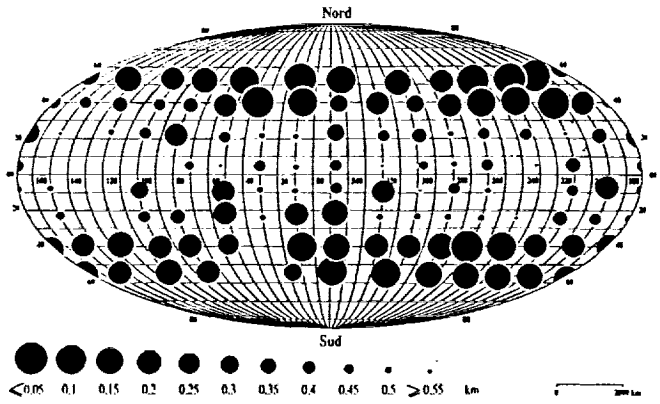

Fig. 1. Distribution of the ground-ice table on Mars.

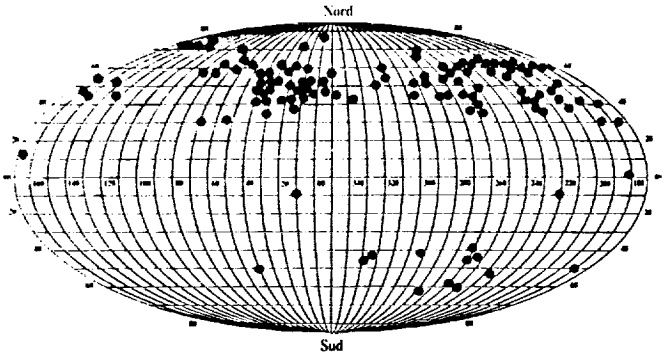

Fig. 2. Distribution of rampart craters less than 1 km in diameter (depth of ground-ice table, < 100 m).

In order to estimate the depth of the ground-ice table, the minimum diameter of impact craters with flow lobes is taken into account [4,5]. On the map (Fig. 1) each 15° × 23° box represents a 1/2.000.000 map Viking photomosaic boundary. The excavation depth of impact craters is in direct relation with crater diameters. A large crater excavates to greater depths than smaller ones and can reach a deeper ground-ice table. The estimation of the relative excavation depth is based on a depth-diameter ratio equal to 1/10 [6,7].

Description: The map (Fig. 1) shows a latitudinal distribution of martian ground-ice with a deep ground-ice table at equatorial latitudes and a subsurface ground-ice table at mid and high latitudes. The top layer of ground-ice is found at a depth exceeding 0.3 km at equatorial latitudes, and of about 150 m for high latitudes. Figure 2 shows the distribution of rampart craters less than 1 km in diameter. The map exhibits a latitudinal control on the distribution of the ground-ice table (less than 100 m deep) between 40° and 75° in latitude.

Interpretation: Correlation with latitudes of martian rampart craters has been previously investigated by several authors [8,9,10,11,12]. Some of these studies suggest the presence of a large amount of ground-ice on Mars, with a near surface ground-ice in the northern plains and a permafrost at low latitude containing a large amount of volatiles at depth.

The map in Fig. 1 shows a discontinuity in the depth of the ground-ice table near 35°–40° latitudes. This discontinuity might

be related to the stability of near surface ground-ice at those latitudes. At latitudes higher than 40° the soil never reaches the frost point during the year, and is therefore in equilibrium with the atmosphere. In such a case, water is always stable as ice. The map confirms the theoretical distribution of volatiles by Fanale et al. [13].

Conclusion: Spatial variations in the spin axis of the planet affect the latitudinal distribution of the Sun's insolation, and therefore the martian ground-ice distribution. Such a latitudinal distribution of ground-ice table suggests that polar wandering [14] has not been so extensive. The observed latitudinal distribution of ground-ice table is in agreement with small variations in the obliquity [15] of Mars (between 15° and 35°), and with a relatively small or short polar wandering. Based upon rampart crater statistics, such stable martian poles on the planet's crust are implied since Hesperian age.

This work was supported by P. N. Planetology of I.N.S.U.

References: [1] Carr M. H. et al. (1977) *JGR, 82*, 4055–4065. [2] Mouginis-Mark P. J. (1979) *JGR, 84*, 8011–8022. [3] Costard F. M. (1989) *Earth, Moon and Planets, 45*, 265–290. [4] Kuzmin R. (1980) *LPSC*, 585–586. [5] Battistini R. (1984) *Earth, Moon and Planets, 31*, 49–61. [6] Boyce J. M. (1979) *NASA TM-80339*, 114–118. [7] Melosh H. J. (1989) In *Impact Cratering: A Geological Process*, Oxford. [8] Johansen L. A. (1979) *NASA TM-80339*, 123–125. [9] Kargel J. S. (1986) *LPSC*, 410–411. [10] Kargel J. S. (1989) *Intl. Conf. on Mars*, Tucson, 132–133. [11] Horner V. M. and Greeley R. (1987) *JGR, 92*, E561–E569. [12] Kuzmin R. et al. (1988) *LPSC*, 657–658. [13] Fanale F. P. et al. (1986) *Icarus, 67*, 1–18. [14] Schultz P. H. (1985) *Sci. Am., 253*, 94–102. [15] Ward A. W. (1974) *JGR, 79*, 3375–3386.

N92-28485

Nature and Evolution of the Early Martian Atmosphere: Evidence from Highland Crater Populations. Robert A. Craddock and Ted A. Maxwell, Center for Earth and Planetary Studies, National Air and Space Museum, Smithsonian Institution, Washington DC 20560, USA.

The initial temperature of Earth's primordial atmosphere is generally agreed to be high. However, ~4.0 b.y. ago the atmospheric and surface temperatures became low enough to allow the oceans to form [1]. Formation of the Earth's core at about the same time also removed free metal from the mantle and crust causing the atmosphere to become less reduced [2]. Similarly, Mars may have also had a primordial, highly reducing steam atmosphere. There is abundant geomorphic evidence to suggest that Mars had a much denser and warmer atmosphere than the one present today. Outflow channels [3], ancient valley networks [4], and degraded impact craters in the highlands [5] all indicate that liquid water was stable on the martian surface at one time. The pressure, composition, and duration of this atmosphere is largely unknown. We have attempted to place some estimates on the nature of the early martian atmosphere by analyzing morphologic variations of highland impact crater populations. This is important for understanding the climatic evolution of Mars, the relative abundance of water on the surface in the past and present, and also the nature of highland surface materials.

In order to avoid influences on crater morphology from variations in the amount of volatiles within the substrate [6], terrain softening [7], and an aeolian blanket which may become thicker at higher latitudes [8] we limited our study to ±30° latitude. We also constrained our study to Noachian cratered (Npl_1) and dissected (Npld) plateau sequences defined by the 1:15M Mars geologic mappers, which allows our results to be easily reproduced. Although a variety of other materials compose the southern cratered highlands, the interpretation of these units includes resurfacing by processes we feel are separable from an earlier global event and, as a result, have not been included in this study. The total area investigated covers over 16.4×10^6 km^2 of the martian cratered highlands, or ~11.3% of the surface area of the planet, and includes 17,497 impact craters greater than 2 km diameter. Crater populations were separated by morphology (degraded vs. fresh) and binned by geology, latitude, and elevation.

Based on the number of superposed fresh impact craters, crater degradation processes ceased entirely on Mars by the end of the Hesperian. Although crater degradation ceased at relatively the same time for both Npl_1 and Npld materials (N[5] = 184±6 and 197±4, respectively), total crater populations suggest that Npl_1 materials may be slightly older (N[5] = 592±10 vs. 521±7 for Npld). However, at diameters >16 km, the size-frequency distribution curves for the two crater populations overlap, suggesting that the materials are actually contemporaneous in age. Perhaps Npl_1 materials preserved slightly more craters with diameters <16 km, or alternatively, degradation processes preferentially eroded smaller diameter craters from the Npld materials (as would be expected from the large number of runoff channels contained in Npld materials).

There appears to be no systematic correlation between resurfacing age and latitude in either of the two geologic units investigated in this study. A very strong correlation does exist, however, between cessation of the crater degradation process and elevation. In both geologic units, populations of fresh impact craters increase with increasing elevation (Fig. 1). This indicates that at higher elevations, crater degradation processes ceased at an earlier time than at lower elevations. At any given elevation the relative ages associated with various crater diameters show that this process did not shut off catastrophically, but decreased in apparent intensity with time. N[16] crater populations suggest that degradation ceased in the late Noachian, while N[5] crater populations suggest the early Hesperian, and N[2] crater populations suggest the late Hesperian. With increasing time and decreasing elevation, it appears progressively smaller diameter crater populations were affected by degradation.

A number of processes have been invoked to explain the morphology of degraded highland impact craters. In our previous work we have argued for fluvial processes—namely rainfall and seepage of groundwater—to explain both the morphology and the size range of the degraded impact craters [5,9]. These processes would be closely coupled to degassing of the primordial atmosphere. Because the early sun is thought to have had a lower luminosity than today [e.g., 10], ~5 bars of CO_2 may have been needed to maintain the ancient martian surface temperature above freezing and to allow liquid water to be stable [11]. Such a dense atmosphere would have allowed cloud condensation to form at high altitudes, causing precipitation to initially fall uniformly throughout the highlands. With time and loss of the atmosphere, higher elevations would have become isolated from crater degradation processes. Eventually only the very lowest portions of the highlands would have had an appreciably thick atmosphere to allow cloud condensation. The possibility that early solar luminosities were higher than today [12] suggests that

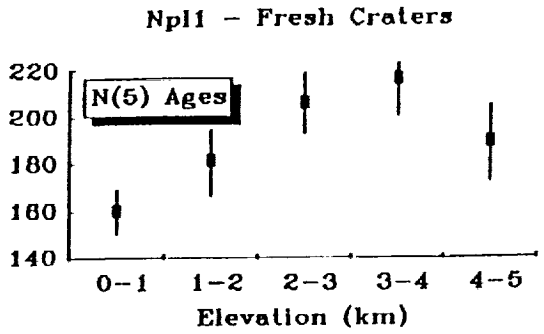

Fig. 1. Age variations for fresh craters in the Noachian cratered plateau sequence (Npl_1) in the martian equatorial highlands. N[5] ages are shown, but similar relationships hold for other crater ages and also for the Noachian dissected plateau sequence (Npld). Highest elevations (4–5 km) have the least counting area.

the early martian atmosphere could have been thinner and still have been warm enough to allow liquid water to exist. However, degassing of a thin atmosphere would also have been quicker, implying extreme rates of highland degradation. Possible recharge of this thin atmosphere through impact-induced CO_2 [13] suggests that highland degradation may have also been periodic. Aeolian erosion and deposition, frequently cited as the other mechanism for crater degradation [e.g., 14], would also be closely coupled to atmospheric degassing.

Release of water in a CO_2-rich atmosphere by precipitation and channel-forming processes has led numerous investigators to speculate on the creation of martian carbonate deposits [e.g., 11]. The formation of such deposits would tend to remove CO_2 from the martian atmosphere and would require a substantially thick primordial atmosphere (~20 bars; [5]) for degradation processes to operate from the middle Noachian to the end of the Hesperian (~450 m.y or ~1.2 b.y.). However, most of these hypotheses have been based on the assumption that an acidic primordial atmosphere (pH <1–3; [15]) was buffered by cations released through the weathering of rock. Precipitation of calcium carbonate occurs only in water with a high pH (>7.8; [16]). On Earth, precipitation of calcium carbonate did not become a common phenomenon until the Proterozoic (2.5 b.y.) when stable, shallow marine cratons developed, thus allowing weathered cations to concentrate [17]. Simply, our oceans were in existence 1.5 b.y. before precipitation of calcium carbonate started to occur, and even then it was in unique circumstances! On Mars water probably was not on the surface in any one place long enough to allow eroded materials to concentrate, raise the pH, and induce the formation of carbonates. This suggests that the martian primordial atmosphere could be thinner (~5 bars) and still allow highland degradation to occur over a long period of time (450 m.y. or 1.2 b.y.).

References: [1] Holland H. D. (1984) *The Chemical Evolution of the Atmosphere and Ocean*, Princeton, 582 pp. [2] Barbato J. P. and Ayer E. A. (1981) *Atmospheres*, Pergamon, 266 pp. [3] Carr M. H. (1986) *Icarus, 68*, 187–216. [4] Pien D. (1980) *Science, 210*, 895–897. [5] Craddock R. A. and Maxwell T. A. (1992) *J. Geophys. Res.*, submitted. [6] Barlow N. G. and Bradley T. L. (1990) *Icarus, 87*, 155–179. [7] Squyres S. W. and Carr M. H. (1986) *Science, 231*, 249–252. [8] Soderblom L. A. et al. (1973) *J. Geophys. Res., 78*, 4117–4122. [9] Craddock R. A. and Maxwell T. A. (1990) *J. Geophys. Res., 95*, 14265–14278 [10] Gough D. O. (1981) *Solar Phys., 74*, 21–34. [11] Pollack J. B. et al. (1987) *Icarus, 71*, 203–224. [12] Graedel T. E. et al. (1991) *Geophys. Res. Lett., 18*, 1881–1884. [13] Carr M. H. (1989) *Icarus, 79*, 311–327. [14] Grant J. A. and Schultz P. H. (1992) *J. Geophys. Res.*, submitted. [15] Ivanov V. V. (1967) *Chemistry of the Earth's Crust, 2*, p. 260, Israel Program for Scientific Translations, Jerusalem. [16] Krumbein W. C. and Garrels R. M. (1952) *J. Geol., 60*, 1–33. [17] Grotzinger J. P. (1989) *Spec. Pub. Soc. Econ. Paleontol. Mineral., 44*, 79.

N92-28486

An Ion Mass Spectrometer for Measuring Isotopic Abundances and Loss Rates of O, C and H in Mars' Upper Atmosphere. R. C. Elphic, B. L. Barraclough, D. J. McComas, and J. E. Nordholt, Space Plasma Physics Group, Los Alamos National Laboratory, Los Alamos NM 87545, USA.

The history of Mars' climate is clearly intimately linked to the evolution of its store of volatiles, particularly H_2O and CO_2. The global CO_2-H_2O system is complex, with a number of production, loss, exchange, and buffering mechanisms operating between the atmosphere and the surface. For example, loss of these volatiles takes place through solar wind interaction with the upper atmosphere/ionosphere, ionospheric chemistry, and through thermal escape. The atmospheric water inventory is, in turn, influenced by exchange with polar water ice deposits and high-latitude ground ice. Atmospheric CO_2, on the other hand, can be lost through adsorption in the regolith and in the formation of carbonates. Finally, oxygen is exchanged between atmospheric CO_2 and H_2O.

Each of these loss and exchange/buffering processes leads to isotopic fractionation; Jakosky [1] has summarized our understanding of the current state of C, H, and O fractionation in the atmosphere (from Earth-based remote sensing and Viking entry probe data) and in the surface (from SNC meteorites). For example, both nonthermal escape processes in the upper atmosphere and formation of carbonates would lead to enhanced atmospheric $^{18}O/^{16}O$, while surface ice condensation would decrease global $^{18}O/^{16}O$. Observations indicate that $\delta^{18}O$ (the permil deviation of $^{18}O/^{16}O$ from the terrestrial standard mean ocean water value) in atmospheric H_2O is –100‰, while $\delta^{18}O$ in atmospheric CO_2 and the SNCs is terrestrial or slightly higher. Loss of oxygen to nonthermal escape processes should produce strong $\delta^{18}O$ enhancement; thus, some dilution of this fractionation must take place, possibly through polar water-ice deposits. Exchange of oxygen between H_2O and CO_2 then provides fractionation between these two species.

Atmospheric carbon isotope fractionation is not well-constrained; $\delta^{13}C$ values range from –50 to +100‰ (Viking) and –70 ± 60‰ (Earth-based), while the SNCs range between +7 and +36‰. While nonthermal atmospheric escape increases $\delta^{13}C$, formation of carbonates reduces it. The observed uncertain level of fractionation is consistent with nonthermal atmospheric loss mitigated by a reasonable surface reservoir of CO_2, probably in the regolith.

Finally, martian atmospheric D/H is enhanced by a factor of 5. If due to thermal loss of H to space, this enhancement corresponds to a loss of most (>85%) of the water in the system [2] in apparent contradiction to the oxygen fractionation. Possibly this

is a reflection of the shorter time scale for H_2O loss (10^5 years); the oxygen fractionation reflects a longer CO_2-H_2O oxygen exchange timescale.

The level of uncertainty in the various isotopic abundances, both atmospheric and surface, leaves the true volatile history an open question. According to Jakosky [1], better estimates of atmospheric oxygen and especially carbon isotopic fractionation will place more stringent constraints on the various scenarios of Mars volatile evolution. Also important are accurate measurements of the loss rates of oxygen and carbon, and how these loss rates may have varied over geologic time. In addition, noble gas isotopic measurements provide insight on physical, as opposed to chemical fractionation. Here we discuss an orbital experiment aimed at addressing these issues.

The Linear Electric Field Time-of-Flight Ion Mass Spectrometer: We describe an approach to obtaining martian upper atmospheric isotopic abundance measurements based on analyzing solar wind-sputtered secondary ions and picked-up photoions with a new technique, a cylindrically symmetric linear electric field (LEF3D) time-of-flight spectrometer. The design is well-developed and mature [3,4]: it is scheduled for flight on NASA's Cassini mission to Saturn, and is presently in advanced prototype testing. A crude prototype of this instrument provided a mass resolution (FWHM m/Δm) of 30; computer simulations indicate that a resolution of much better than 100 is possible. More importantly for isotopic studies. the instrument can be detuned in such a way that molecular ions are separated from atomic ions of the same mass (eg., H_2O^+ vs. $^{18}O^+$).

Our new technique, based on the motion of ions in a region of linear electric field (LEF), is quite simple. For a z-directed electric field $E_z(z)$ which increases linearly with distance along the axis, z, $E_z(z) = -kz$, where k is a constant solely dependent upon the electromechanical configuration of the device. Since the electrostatic force on a particle is qE, where q is the particle charge, the equation of motion for the particle in the z-direction is that of a simple harmonic oscillator of mass m. A particle entering the LEF region at z=0 will return to the z=0 plane after completing half of an oscillation cycle, i.e. when $t = \pi/\omega = \pi\,(m/qk)^{1/2}$.

This timing is accomplished by passing the arriving ions through an ultrathin carbon foil; secondary electrons produced at the foil are accelerated in the LEF region to a detector that starts a timing clock. Positive ions emerging from the foil enter the LEF region and are reflected as described above, and are counted at a second detector which provides the stop signal for that ion's time-of-flight.

However, another feature of the mass spectrometer described here is more important for the Mars isotopic measurements and involves the analysis of molecular ion species. In addition to providing start timing pulses, the carbon foil also dissociates molecular ions. All ions are electrostatically energy-selected and arrive at the foil with a known energy/charge. Passing through the foil, it is dissociated into fragments that all travel with nearly the same velocity so that the energy is partitioned in proportion to the mass of each fragment. These fragments then have less E/q than the initial molecular value and will not travel as deeply into the LEF region of the device as would directly analyzed atomic ions of the same nominal E/q. Because of small E-field nonlinearities in an appropriately detuned LEF3D device, especially at the low-potential entrance end of the device, the times-of-flight of the fragments can be made shorter than those of atomic ions,

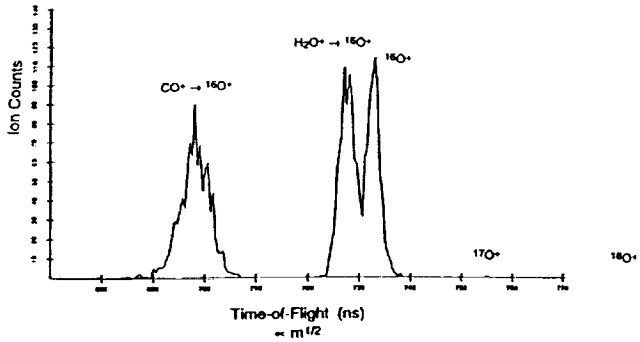

Fig. 1. Time-of-flight ion mass spectrum showing the location of $^{16}O^+$ due to incoming CO^+, H_2O^+ and $^{16}O+$. Locations for isotopic $^{17}O^+$ and $^{18}O^+$ are shown, distinct from the other species.

an effect that allows separation of molecular and atomic interferences.

Figure 1 displays separate peaks for ^{16}O derived from incoming CO^+, H_2O^+, and $^{16}O^+$. Also shown are the calculated locations for incoming atomic $^{17}O^+$ and $^{18}O^+$. The latter locations are distinct from any of the other ions or fragments, and should allow clear detection of the isotopes. With $^{18}O/^{16}O \sim 0.2\%$, 10^5 $^{16}O^+$ counts will be accompanied by 200 ± 14 $^{18}O^+$ counts, providing about 7% statistical uncertainty. Similar results will obtain for the carbon isotopes; establishing the atmospheric $^{12}C/^{13}C$ value to 10% statistical uncertainty or better will be straightforward. $^{15}N/^{14}N$, while less crucial than the fractions of oxygen and carbon isotopes, will also be measurable. Finally, it is possible to distinguish H_2^+ from D^+ with this design, and a measurement of atmospheric D/H should be possible. By measuring these ions as they are removed from the atmosphere, loss rates due to solar wind processes can be established. Together, these measurements should place stringent limits on atmospheric isotopic ratios and improve understanding of Mars' volatile history.

References: [1] Jakosky B. M. (1991) *Icarus, 94*, 14–31. [2] Toon O. B. et al. (1980) *Icarus, 44*, 552–607. [3] McComas D. J. et al. (1990) *Rev. Sci. Instrum., 61*, 3095. [4] McComas D. J. et al. (1990) *Proc. Natl. Acad. Sci. USA, 87*, 5925.

N92-28487

Chemical Models of Volcanic Outgassing on Mars.

Bruce Fegley Jr., Department of Earth and Planetary Sciences and McDonnell Center for the Space Sciences, Washington University, St. Louis MO 63130, USA.

Introduction: During the MSATT workshop in Boulder, CO, several participants emphasized the importance of constraints on the composition and temporal evolution of outgassed volatiles on Mars. In this abstract I present the results of some preliminary calculations that model the composition of volcanic gases as a function of temperature, pressure, oxygen fugacity, and quench temperature. These results can be used in combination with cosmochemical models for the accretion of Mars to assess the plausibility of different atmospheric compositions during the planet's early history.

Computational Methods: The calculations were done with the TOP20 code, which uses the dual constraints of mass balance and chemical equilibrium to iteratively solve for the molecular

composition of a gas having a specified temperature, pressure, and elemental composition [1]. This code contains ~500 compounds of 25 elements (H, C, O, N, S, Cl, F, P, Si, Fe, Mg, Al, Ca, Na, Ni, Ti, Cr, Mn, Co, Zn, Cu, V, K, Br, I). The thermodynamic data used are mainly from the JANAF Tables [2] and an analogous set of tables issued by the (then) Soviet Academy of Sciences [3]. Ideal gas chemical equilibrium calculations were done from 500 K to 2000 K at a pressure of 1 bar. This pressure is consistent with independent estimates of the atmospheric pressure on early Mars. However, the results of the chemical equilibrium calculations are generally more sensitive to temperature than to the assumed total pressure.

Volcanic Gas Model: The preliminary calculations presented here are done by taking a terrestrial volcanic gas composition as a starting point, and then altering the oxygen elemental abundance of this composition to make it more or less reducing. The abundances of the other elements involved are held constant. The chemistry of the volcanic gas is then calculated as a function of temperature at constant pressure. The range of temperatures considered spans plausible magmatic conditions and is extrapolated to both higher and lower temperatures to illustrate trends.

The volcanic gas model chosen for the preliminary calculations is the average composition of volcanic gases collected by Gerlach and Graeber in January 1983 during an eruption on the east rift of Kilauea [4]. These high quality analyses have the following average composition: 80.4% H_2O, 3.7% CO_2, 13.6% SO_2, 1.0% H_2S, 0.16% HCl, 0.18% HF, 0.9% H_2, and 0.07% CO. Gerlach and Graeber [4] noted that the equilibration temperature (here called the quench temperature) for their samples was in the range of 950–1030°C (1223–1303 K). The average molecular composition was then recalculated in terms of the elemental abundances and served as the baseline model for the results described below.

Computational Results: Figure 1 illustrates the major species in the H-C-O-S-F-Cl system as a function of temperature for the average Kilauea volcanic gas composition. The abundances of the different gases are expressed as mole fractions, which are equal to the partial pressure of a gas divided by the total pressure. Figure 2 illustrates the oxygen fugacity for the average Kilauea volcanic gas as a function of temperature and compares it to the oxygen fugacities buffered by different coexisting mineral assemblages. The abbreviations represent the following minerals: M = magnetite Fe_3O_4, H = hematite Fe_2O_3, Q= quartz SiO_2, W = wüstite FeO, and I = iron metal. These results illustrate several important points. First, the calculations reproduce the input composition at the quench temperature. This confirms the results of Gerlach and Graeber [4]. Second, we also confirm that the oxygen fugacity at the quench temperature is close to that of the QFM buffer. As the gas phase cools it becomes much more oxidizing if it evolves as a closed system, i.e., if it is no longer buffered by mineral assemblages in the magma. This is reflected by the decreasing abundances of CO and H_2 with decreasing temperature (see Fig. 1). However, at the same time, reduced sulfur gases such as H_2S and elemental sulfur vapor become increasing important.

Figure 3 illustrates the results of varying the oxygen fugacity at constant temperature and pressure. A temperature of 1300 K, consistent with the quench temperature for the Kilauea volcanic gases, was used here, and the total pressure is one bar. This figure is a vertical slice through Fig. 2. It shows that as the volcanic gas composition becomes more reducing that H_2, CO, and H_2S

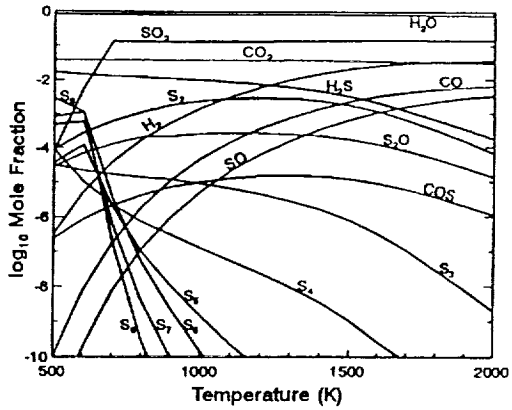

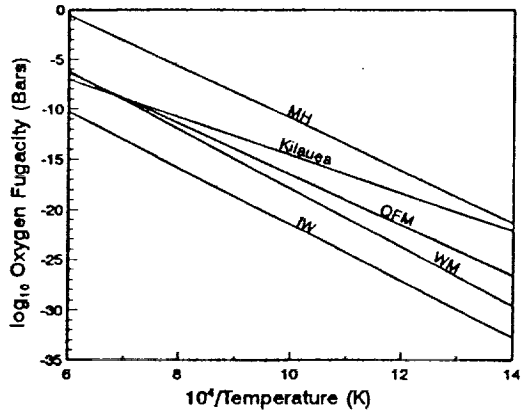

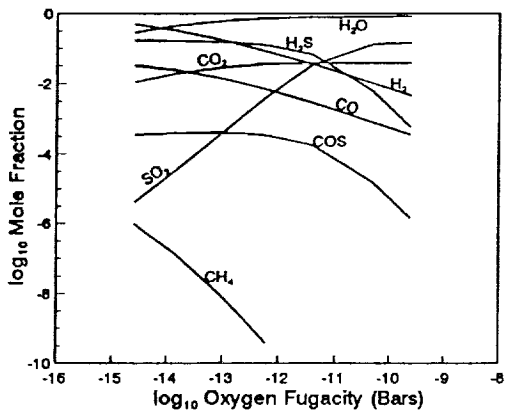

become more important relative to their oxidized counterparts and finally become dominant at oxygen fugacities around IW. In contrast, methane remains a minor species, although its abundance does increase. As the gas composition becomes more oxidizing, trending towards MH, the major gases remain the same as in the Kilauea samples. At sufficiently high oxygen fugacities, SO_3 may become important, but not in a cosmochemically reasonable environment.

Implications for Mars: The most reduced conditions that are plausible on early Mars would be at the IW buffer. The accretion of reduced material containing metallic iron is necessary to do this, and is not predicted in all cosmochemical models. Even under these conditions, the outgassed volatiles probably contain most carbon as CO and CO_2 with very little CH_4. Nitrogen, not

included here because all N in volcanic gases is plausibly explained by contamination, would remain as N_2 because NH_3 is unstable at such a high quench temperature. Sulfur is mainly as H_2S. As an initial reduced assemblage evolves (e.g., iron metal sinks to a core and/or reacts away), the outgassed volatiles will become more oxidized and will come to resemble present-day volcanic gases. Thus, these preliminary calculations predict a predominantly CO_2, N_2, water vapor composition for early martian volatiles. Sulfur will possibly be present as SO_2, although this is by no means certain.

Acknowledgments: This work was supported by the NASA Planetary Atmospheres Program.

References: [1] S. S. Barshay and J. S. Lewis (1985) *Icarus, 33*, 593–611. [2] *JANAF Thermochemical Tables, 3rd edition* (1985) ACS-APS, Washington, D.C. [3] *Thermodynamic Properties of Individual Substances* (1978–1982) High Temperature Institute, Moscow. [4] Gerlach T. M. and Graeber E. J. (1985) *Nature, 313*, 273–277.

N92-28488

Redistribution of Subsurface Neutrons Caused by Ground Ice on Mars. W. C. Feldman[1], W. V. Boynton[2], B. M. Jakosky[3], and M. T. Mellon[3], [1]Los Alamos National Laboratory, Los Alamos NM 87545, USA, [2]University of Arizona, Tucson AZ 85718, USA, [3]Laboratory for Atmospheric and Space Physics and Department of Geological Sciences, University of Colorado, Boulder CO 80309-0392, USA.

Introduction: A recent study of the stability of ground ice on Mars [1] showed that long-term contact with the atmosphere should result in a relatively thick layer of buried ground ice wherever the mean annual surface and subsurface temperature is below the atmospheric frost point. This situation generally obtains poleward of 40 to 50° latitude. According to their calculations, the equivalent water content of such deposits should vary up to the maximum allowed by the pore size of the regolith, about 0.37 g/cm^3. This value amounts to a water mass fraction of 18% assuming a regolith density of 1.65 g/cm^3. Burial depths below the atmosphere-regolith interface ranged between about 20 and 100 g/cm^2 depending upon the mean annual temperature and temperature variation experienced by the surface. The bottom edge of the deposit ranged down to about 300 g/cm^2, depending on the depth where the geothermal gradient begins to dominate the regolith temperature structure. This study was part of an ongoing effort to determine the ability of the Mars Observer Gamma-Ray Spectrometer (MOGRS) to detect and quantify the distribution of near-surface ground ice on Mars.

Previous studies of neutron energy distributions in equilibrium with a variety of regolith chemistries and stratigraphies (e.g., [2] and references therein) revealed a remarkably strong sensitivity and specificity. In particular, an increase in the water content of an assumed infinitely thick regolith from 0 to about 10% by mass increases the neutron flux in the thermal energy range while decreasing the flux in the epithermal energy range. The net effect on the thermal to epithermal flux ratio amounts to more than an order of magnitude at all depths while moving the depth at which the thermal flux maximizes closer to the surface [3,4]. Production rates of neutroncapture gamma rays should follow the neutron thermal flux thereby increasing in magnitude at all depths while concentrating closer to the surface [5]. These effects are sufficiently large that they should be detectable from orbit using the MOGRS. Indeed, a recent comprehensive study of the combined effect on planetary leakage gamma rays and neutrons, of a variety of soil-ice mixing geometries, revealed major effects on the predicted spectra that should thereby allow detailed geochemical interpretations [6]. The purpose of the present study is to build on that of Squyres and Evans to approach the specific problem of the buried ice deposits explored by Mellon and Jakosky [1]. We therefore calculated the depth dependence of equilibrium neutron energy spectra and related neutron-capture gamma-ray production rates for a semi-infinite layer of regolith having a Chryse-fines composition [7] containing 5, 10, and 18 wt% of water. This high water-content layer was buried beneath the same regolith containing 1% water at depths of 20, 40, and 80 g/cm^2. A 16-g/cm^2 atmosphere having the abundances measured by Owen et al. [8] was included throughout. We also calculated the effects of a 30-g/cm^2-thick layer containing 18% water embedded within a semi-infinite regolith containing 1% water, at depths of 20, 40, and 80 g/cm^2 below the atmosphere-surface interface.

Results: The different energy regions of calculated neutron spectra were quantified in this study in terms of the known response of practical neutron detectors. We therefore chose the epithermal neutron band to consist of the response of a cadmium-wrapped, 5-cm-diameter gas proportional counter filled with 10 atm of ^{3}He, the thermal band to be the count-rate difference between a bare and a cadmium-wrapped ^{3}He counter, and two fast neutron bands with ranges between 0.5 and 1.5 MeV, and between 1.5 and 10 MeV, respectively. We found marked redistributions of neutrons with depth for each of these models and for each of the four neutron bands. As expected, the neutron-capture gamma ray production rate followed the flux of the thermal neutrons and was likewise redistributed in depth. In addition to the effects reported previously [3], the thermal neutrons were generally concentrated into the region of enhanced water across the surface interface separating it from the 1% regolith. This effect caused a localized large build-up just below the interface and a corresponding deficit above the interface. On the other hand, all three of the other bands decreased across the interface by an amount that became less pronounced and less sharply defined, with increasing neutron energy. The effects observed in the epithermal band began to mix with that in the thermal band when the interface moved toward the martian surface. Additional calculations showed that this effect was due to a combination of the effects of the atmosphere and to the operational definition of the epithermal neutron band adopted here. This last effect therefore needs to be included in interpretations of measured datasets when they become available.

Similar results were obtained for the simulations of a 30-g/cm^2-thick, high water-content layer embedded within a semi-infinite low water-content layer. Here, thermal neutrons were leached out of both higher and lower neighboring low water-content layers into the high water-content layer. Neutrons in all other energy bands were reduced moderately in neighboring layers and sharply reduced in the high water-content layer. Graphical results of our simulations will be presented at the meeting.

References: [1] Mellon M. T. and Jakosky B. M. (1992) *JGR*, submitted. [2] Feldman W. C. et al. (1992) in *Remote Geochemical Analysis: Elemental and Mineralogical Composition* (C. M. Pieters and P. J. Englert, eds.), in press. [3] Lapides J. R. (1981) Ph.D. dissertation, Univ. of Maryland,

College Park. [4] Drake D. M. et al. (1988) *JGR, 93*, 6353. [5] Feldman W. C. et al. (1989) *JGR, 94*, 513. [6] Squyres S. W. and Evans L. G. (1992) *JGR*, submitted. [7] Toulmin P. A. et al. (1977) *JGR, 82*, 4625. [8] Owen T. et al. (1977) *JGR, 82*, 4635.

Time Variation of the Meteoritic Contribution to the Atmosphere of Mars. G. J. Flynn, Department of Physics, State University of New York–Plattsburgh, Plattsburgh NY 12901, USA.

In the present era meteoritic material is known to make a significant contribution to the atmosphere of the Earth. Direct collection from the Earth's stratosphere has established that surviving micrometeorites are the major naturally occurring particle >1 μm in diameter at 20 km [1]. The effects on the Earth's atmospheric chemistry of meteoric metal vapors (Fe, Ni, Na, K, Mg, and Ca) and the particulates which recondense in meteor vapor trails were examined by Turco et al. [2], who concluded that 1) meteoric debris may dominate the <0.01 μm aerosols above 20 km, 2) important chemical reactions are likely to occur of the surfaces of stratospheric particles, and 3) metallic elements derived from ablating meteorites may significantly neutralize sulfuric acid in the Earth's stratosphere. In a similar manner, meteoritic material may have significant effects on the chemistry, dust load, and radiational energy balance of the atmosphere of Mars. The present contribution of meteoritic material to the atmosphere of Mars has been estimated to total 12×10^6 kg/year [3], about 75% of the 16×10^6 kg/year measured at Earth [4]. Of this, surviving micrometeorites are estimated to contribute 8.6×10^6 kg/year in the range from 1 to 1200 μm, with recondensed meteoric vapor supplying up to 2.4×10^6 kg/year of particles ≤1 μm [3].

This meteoritic contribution to the planets of the inner solar system varies significantly with time. During the first billion years the flux of meteoritic material was significantly greater than at present. Over the past 3.6 b.y. the background flux has been relatively constant, but shorter periods of significantly enhanced flux are associated with discrete events such as major impacts of large bodies onto the planets or their moons and passage through cometary debris streams.

First Billion Years: Over the long term (on a timescale of tens of million years) the contribution of meteoritic material to the lunar soils has been fit by a two component model consisting of an early, short-lived meteoritic component ($t_{1/2}$ = 40 m.y.) with a very high initial flux (10^3 to 10^7 times the present flux [5]), and a relatively constant accretion of 2.9 g/cm^2 b.y. of meteoritic material over the past 3.6 b.y. [5]. Although the size distribution of this early meteoritic flux is not known, the meteoritic component is likely to have played a substantial role in determining the optical transparency, radiational energy balance, chemical properties, and particulate load of the early atmosphere of Mars.

Last 3.6 Billion Years: Although the long-term average meteoritic flux at the Moon (and presumably the inner solar system) has been relatively constant over the past 3.6 b.y., the average value of that flux may have been substantially higher than the value determined from present measurements. Hughes [4] reports a current meteoritic accretion at Earth to be 16×10^6 kg/year. However, Kyte and Wasson infer a higher meteoritic accretion rate at Earth, 78×10^6 kg/year, from iridium concentrations in Pacific sediments [6], consistent with an earlier value of 110×10^6 kg/year for Pacific sediments obtained by Shedlowsky and Paisley [7]. The inferred long-term meteoritic accretion rate on the Moon, adjusted for the near-Earth gravitational flux enhancement of 2.4 [8], leads to a meteoritic accretion rate at Earth of about 40×10^6 kg/year. Thus the long term meteoritic flux in the inner solar system may be a factor of 2.5 to 5 times higher than the current flux, which was used in to estimate the current accretion of 12×10^6 kg/year of meteoritic material onto Mars [4].

There are a number of effects which may give rise to large, short-term (~days to decades) variations in the flux of meteoritic material at Earth and Mars. The importance of these discrete events on the atmosphere of Mars can be assessed by comparison of their meteoritic input with the 12×10^6 kg/year continuous meteoritic input.

Large Impacts: Kyte and Wasson [6] reported a large iridium spike (not included in their average) in the Pacific sediment, consistent with a major meteoritic impact event at the K-T boundary discovered by Alverez et al. [9]. Although large objects (preatmospheric mass >1 kg) reach the surface of the Earth as meteorites without depositing a large fraction of their mass in the atmosphere, kilometer-sized objects, such as the one suspected to have occurred at the K-T boundary [9] can produce sufficient ejecta to contaminate the Earth's atmosphere for years, altering the global radiational balance. Such large impacts have a reasonable probability of occurrence: 10^{18} g (~18 km diameter) once every 2×10^9 years, 10^{17} g (~9 km) once every 10^8 years, 10^{16} g (~4 km) once every 3×10^6 years at Earth. Since the flux of large objects at Mars is estimated to be 2.6 times the Earth impact rate [10], major impacts events having global environmental consequences are likely to have occurred frequently over the history of Mars. In the present atmosphere of Mars the residence time of the ejected dust will be much shorter than for Earth, but in periods of increased atmospheric density longer dust residence would be expected.

Passage Through Comet Tail: The flux of meteors in the showers associated with active comets varies from year to year, depending on the relative position of the comet and the Earth during the shower. Whipple [11] has suggested that, in the past, some comets may have been significantly more active in emitting dust than in the present era. Although, at present, the dust emission from all active, short-period comets is only sufficient to account for a few percent of the dust required to maintain the zodiacal cloud in equilibrium, Whipple [11] proposed that an active phase in the evolution of Comet Encke might supply the required dust. This would require Comet Encke to emit 50 times more dust than at present. Direct passage through the tail of an active comet, particularly one as active as Whipple has suggested for the early phase of Encke, has the potential for significantly enhanced dust flux.

Major Collision in the Main-Belt: Sykes and Greenberg [12] have suggested that the belts of enhanced infrared emission in the asteroid belt may result from infrequent, catastrophic disruptions of major asteroids. The existence of asteroid "families," presumed to be fragments from such disruptions, supports this idea. Small debris (<100 μm in size) from these catastrophic disruptions would be transported from the main belt to a Mars-crossing orbit on a short timescale, a few hundred years for 1-μm particles and less for smaller material, resulting in an increased flux of meteoritic material following a major collision in the main belt.

The proximity of Mars to the inner edge of the main belt would make this a more important effect at Mars than at Earth.

Material from the Martian Moons: Although Phobos and Deimos are small compared to the Moon, the surfaces of these moons can also serve as important, short-term contributors of dust to the atmosphere of Mars.

Impacts onto the surfaces of Phobos and Deimos excavate a large amount of debris, most of which is initially injected into orbits around Mars or is captured by the atmosphere. The impact event which formed the 11-km-diameter crater Stickney, the largest crater on Phobos, is likely to have produced ~10^{14} kg of ejecta. Even if only a small fraction of this ejecta were added to the Mars atmosphere it would exceed the 12×10^6 kg/year contribution from interplanetary dust. The dust ring produced by the material not captured by the atmosphere might also have environmental consequences, as described by O'Keefe [13] for the terrestrial case.

Ruderman and Truran [14] have suggested that dust ejected from the Moon by a supernova gamma ray flash could cause sudden climatic changes on Earth by vaporizing lunar surface material and depositing it in the atmosphere of the Earth. A gamma ray flash of the magnitude expected once every 10^8 years could vaporize about 1 g/cm^2 on the Moon's surface in less than 1 sec (14). This would vaporize ~7×10^9 kg of material from the surfaces of the Martian moons, potentially exceeding the present annual contribution of meteoritic material to Mars by three orders of magnitude.

There are a number of mechanisms that are known or proposed to inject substantial quantities of material into the atmosphere of the Earth. Similar mechanisms must also operate on Mars, and these mechanisms have the potential to alter the atmospheric opacity, chemistry, and dust content causing significant, short-term climatic consequences for the planet.

References: [1] Fraundorf P. et al. (1982) in *Comets* (L. Wilkening, ed.), Univ. of Ariz., 383–409. [2] Turco et al. (1981) *JGR, 86*, 1113–1128. [3] Flynn G. J. (1992) *LPSC XXIII*, 371–372. [4] Hughes D. (1978) in *Cosmic Dust* (J.A.M. McDonnell, ed.), Wiley, 123–185. [5] Wasson J. T. et al. (1975) *Moon, 13*, 121–141. [6] Kyte F. and Wasson J. T. (1986) *Science, 232*, 1225–1229. [7] Shedlowsky J. P. and Paisley S. (1966) *Tellus, 18*, 499–503. [8] Grew G. W. and Gurtler C. A. (1971) *NASA TND–6266*, 1–44. [9] Alverez I. W. et al. (1980) *Science, 237*, 56–58. [10] Shoemaker E. M. (1977) in *Impact and Explosion Cratering* (D. J. Roddy et al., eds.), Pergamon, 617–628. [11] Whipple F. L. (1967) in *The Zodical Light and the Interplanetary Medium*, NASA SP-140, 409. [12] Sykes M. V. and Greenberg R. (1986) *Icarus, 65*, 51–69. [13] O'Keefe J. A. (1980) *Nature, 285*, 309–311. [14] Ruderman M. and Truran J. W. (1980) *Nature, 284*, 328–329.

The Production and Escape of Nitrogen Atoms on Mars. J. L. Fox, Institute for Terrestrial and Planetary Atmospheres, State University of New York at Stony Brook, Stony Brook NY 11794, USA.

The lack of agreement between our previously computed values and those measured by Viking of the ^{15}N:^{14}N isotope enhancement ratio [1] has led us to reevaluate our model [2] of the martian ionosphere. In previous models, we were unable to reproduce the ion profiles measured by the RPA on Viking using electron temperatures that were higher than the ion temperatures [2,3]. Recently Hanson and Mantas [4] used the Viking RPA data to derive electron temperatures for altitudes greater than 200 km, and the reported values of 2500 to 3000 K are larger than the ion temperatures by a factor that varies from about 4 at 200 km to about 50% at 300 km. When we increased the electron temperatures to these values, and with a zero flux upper boundary condition, the ion densities at high altitudes exceeded the measured values by a large factor. Shinagawa and Cravens [5] constructed a one-dimensional magnetohydrodynamic model of the martian ionosphere and found that the measured profiles could be best fit if a loss process were imposed at the top of the atmosphere. They proposed that this loss was due to the divergence of the horizontal fluxes. We also have found that we can better fit the observed profiles if we impose a loss process at the upper boundary of our model. If the horizontal fluxes of ions do not constitute a net loss of ions (for example, by converging and flowing downward on the nightside), then the escape of N due to dissociative recombination is also inhibited, and better agreement with the measured isotope ratio is found.

The production of escaping nitrogen atoms is closely related to the production of thermospheric odd nitrogen and therefore the densities of NO measured by Viking [6] provide a convenient check on our nitrogen escape model. Our standard model NO densities are less than the measured values by a factor of 2–3, as are those of previous models [7,8]. McElroy et al. [7] obtained agreement between the measured and model NO profiles by increasing the cross sections for electron-impact dissociation of N_2 measured by Winters [9] by a factor of five below 40 eV. The cross sections of Winters, however, have been shown by Zipf and McLaughlin [10] to be correct. We find that reasonable agreement can be obtained by assuming that the rate coefficient for loss of odd nitrogen in the reaction of N with NO is smaller at temperatures that prevail in the lower martian thermosphere (about 130–160 K) than the standard value, which applies to temperatures of 200–400 K [11]. Since this correction applies to the loss of odd nitrogen rather than to its production, the N escape rates are not affected.

TABLE 1. Computed ^{14}N escape fluxes.

Process	Escape Flux (10^5cm^{-2}s^{-1})		
	Low SA[a]	High SA[a]	Average
$N_2 + h\nu \rightarrow N + N$	0.59	1.4	1.0
$N_2 + h\nu \rightarrow N^+ + N + e$	0.17	0.60	0.39
$N_2 + e \rightarrow N^+ + N + 2e$	0.14	0.48	0.31
$N_2^+ + O \rightarrow NO^+ + N$	0.44	1.33	0.89
$O^{++} + N_2 \rightarrow N^+ + N + O^+$	0.059	0.17	0.11
$N_2^+ + e \rightarrow N + N$	0.51	3.5	2.0
Total	1.9	7.5	4.7

a. Solar Activity

The ^{14}N escape fluxes for our revised ionospheric model are shown in Table 1. Integrating backward in time, taking care to account for the increase in the altitudes of the exobase and homopause, and the changes in the fluxes due to changes in the composition of the atmosphere, we find an isotope enhancement ratio and an initial column density of about 2.6 and 1.0×10^{23} cm^{-2}, respectively, when theoretical data are employed for the

yields of the channels in dissociative recombination [12]. The existence of a dense early atmosphere is consistent with this model. If the initial CO_2 pressure is assumed to be 2 bars, exponential loss of the atmosphere with a time constant of about 2.2×10^{16} s (7×10^8 yr) reproduces the measured isotope ratio.

References: [1] Nier A. O. et al. (1976) *Science, 194*, 68. [2] Fox J. L. and Dalgarno A. (1983) *JGR, 88*, 9027. [3] Fox J. L. (1992) In *Workshop on The Martian Surface and Atmosphere Through Time*, pp. 53–54, LPI, Houston. [4] Hanson W. B. and Mantas G. P. (1988) *JGR, 93*, 7538. [5] Shinagawa H. and Cravens T. E. (1988) *JGR, 94*, 6506. Also (1992) *JGR, 97*, 1027. [6] Nier A. O. and McElroy M. B. (1976) *JGR, 82*, 4341. [7] McElroy M. B. et al. (1977) *JGR, 82*, 4379. [8] Krasnopolsky V. A. (1992) *Icarus*, in press. [9] Winters H. F. (1966) *J. Chem. Phys., 44*, 1472. [10] Zipf E. C. and McLaughlin R. W. (1978) *Planet. Space Sci., 26*, 449. [11] Atkinson R. et al. (1989) *J. Phys. Chem. Ref. Data., Supplement III, 18*, 881. [12] Guberman S. L. (1991) *Geophys. Res. Lett., 18*, 1051.

N92-28491

High Pressure Experiments with a Mars General Circulation Model. R. M. Haberle, J. B. Pollack, J. R. Murphy, J. Schaeffer, and H. Lee, NASA Ames Research Center, Moffett Field CA 94035-1000, USA.

If Mars did start out with a high-pressure CO_2 atmosphere, then it is likely it did not have polar caps like it does today. Venus, for example, has a 90-bar CO_2 atmosphere and no polar caps. Mars may not have begun with such a massive atmosphere, but it almost certainly had more of an atmosphere than it does today (7.5 mb). And if it started out with as much as 1 bar of CO_2, then it probably didn't have polar caps. An important question therefore, is: At what point during the evolution of Mars' atmosphere did its polar caps begin to form?

The answer to this question may have some bearing on the "warm early Mars" model. Kasting [1] has shown that the condensation of CO_2 in the atmosphere—something not considered in previous climate models—inhibits the greenhouse effect and that no amount of CO_2 can maintain a globally averaged surface temperature of 273 K prior to about 3 b.y. ago. However, if there is a substantial latitudinal gradient in surface temperature, then it's possible that the surface temperature was below freezing in the global mean, but at or above freezing in the tropics. If the gradient is steep enough to satisfy the global mean constraint, but not so steep that CO_2 condenses in the polar regions, then there might not be a need to search for additional greenhouse gases as Kasting suggests.

However, this may be a tall order for the circulation. According to Kasting's results, the globally averaged surface temperature must have been well below 253 K for the first billion years or so (if Mars had a pure CO_2 atmosphere). Suppose, for example, the mean surface temperature was 240 K. Then if the tropics are to be at the melting point (~270 K) then the atmosphere must transport enough heat to keep the poles at about 210 K—almost 60 K warmer than they are today! (This is just a crude estimate, but it does illustrate the point).

Gierasch and Toon [2] constructed a simple energy balance model that predicted the polar caps would disappear if the surface pressure was increased to roughly 200 mb. Heat transport into the polar regions increases with surface pressure and becomes sufficient to vaporize the caps at 200 mb. More recently, McKay et al. [3] calculate even lower surface pressures (~100 mb) are sufficient to eliminate the caps because the greenhouse effect, which was ignored by Gierasch and Toon, provides an additional heat source.

Note that in both approaches the poleward heat flux by the atmosphere was parameterized using Stone's [4] baroclinic adjustment theory. This theory assumes that the heat flux is carried by large-scale zonally asymmetric wave motions that arise from the (baroclinic) instability of the mean zonal wind field. The Mars General Circulation Model (GCM) of Pollack et al. [5] indicates that this component may not be as important as the mean meridional circulation, though it does play a role. Furthermore, Gierasch and Toon assumed the heat flux maximized at 45° and decreased uniformly with latitude between there and the pole. Again, the GCM indicates otherwise (e.g., the heating is concentrated near the edge of the polar cap).

The interaction of three physical processes will determine the stability of the polar caps as the surface pressure increases: the greenhouse effect, atmospheric heat transport, and the change in the CO_2 frost point temperature. The contribution of each is readily determined in the GCM. Therefore, we have initiated experiments with the GCM to determine how these processes interact, and how the atmosphere-polar cap system responds to increasing surface pressure. The experiments are carried out for northern winter solstice and generally assume the atmosphere to be free of dust. Each experiment starts from resting isothermal conditions and runs for 50 Mars days. Mars' current orbital parameters are used. The experiments are for surface pressures of 120, 480, and 960 mb, which represent 16, 64, and 128 times the current value.

To date we have analyzed the 120 mb experiment and the results indicate that contrary to the simpler models, the polar caps actually advance instead of retreat. Compared to a run in which the initial surface pressure is 7.5 mb, the polar cap boundary moves from 41.3° N to 33.8° N—an almost 50% increase in surface area! Furthermore, CO_2 appears to occasionally condense at latitudes as far south as the equator and even into the southern hemisphere. The reason the caps expand in this experiment is due to the fact that the frost point temperature at 120 mb is about 170 K, almost 20 K greater than it is at 7.5 mb. To prevent polar cap formation, therefore, the combined effects of the greenhouse effect and atmospheric heat transport must provide this much heating. However, in this simulation they do not: the greenhouse effect is only marginally strengthened, and heat transport is unable to make up the difference. Thus, the polar caps expand.

Of course, there must be some point at which the greenhouse effect and heat transport become strong enough to overcome the frost point increase. The purpose of the 480 and 960 mb experiments is to determine where this transition occurs and, more importantly, to determine if polar caps form and if mean surface temperatures reach the melting point. However, the key to these experiments is the greenhouse effect, which at these higher pressures will be mostly due to water vapor. This important greenhouse gas is not presently accounted for in the GCM. Instead, we use the model's dust heating algorithms as a proxy. This is done by varying the ratio of the dust visible-to-infrared optical depth. These experiments have yet to be analyzed, but will be reported on at the workshop.

A particularly intriguing result of the 120 mb experiment is its predictions regarding CO_2 clouds. These clouds form not only in the winter polar regions—where they usually form for current

conditions (see [5])—but also in the tropics and midlatitudes of both hemispheres. As Kasting points out, CO_2 clouds can further decrease the greenhouse effect and, in this case, further the tendency for glaciation. The radiative effects of these clouds are not accounted for in the GCM. However, in the 120 mb simulation, surface stresses are significantly increased over their values at 7.5 mb and dust lifting appears likely. If dust is lifted to the altitudes that the CO_2 clouds form (15–60 km), their heating effects may prevent condensation. Thus, the role of these clouds on the evolution of the atmosphere cap system remains uncertain.

References: [1] Kasting J. F. (1991) *Icarus, 94*, 1–13. [2] Gierasch P. J. and Toon O. B. (1973) *J. Atmos. Sci.*, 1502–1508. [3] McKay C. P. et al. (1991) *Nature*, 489–496. [4] Stone P. H. (1972) *J. Atmos. Sci.*, 405–518. [5] Pollack J. B. et al. (1990) *JGR, 95*, 1447–1474.

N92-28492

Mars Volatile Evolution: Implications of the Recent Measurement of ^{17}O in Water from the SNC Meteorites.

Bruce M. Jakosky, Laboratory for Atmospheric and Space Physics and Department of Geological Sciences, University of Colorado, Boulder CO 80309-0392, USA.

Oxygen, carbon, and hydrogen isotopes in water and carbon dioxide in the martian environment can fractionate due to processes involving escape to space, exchange between atmospheric and non-atmospheric species, and exchange of atoms between different molecules. As a result, the ratios of $^{18}O/^{17}O/^{16}O$, $^{13}C/^{12}C$ and D/H in atmospheric and surface species are sensitive indicators of the integrated effects of outgassing and volatile evolution over geologic time. In a 1991 paper in Icarus, I summarized all of the available observations of isotopic abundances and compared them with models of fractionation in order to see which scenarios of volatile evolution were most plausible. Since then, Karlsson et al. (1992) have reported measurements of ^{17}O in water trapped within the SNC meteorites (the SNC meteorites are thought to be pieces ejected from the martian surface). Their value of $\Delta^{17}O$ (see below) was several tenths of a ‰ greater than that of the oxygen contained within the silicate minerals, suggesting that the water had evolved separately from the silicates prior to the ejection from the martian surface. I have now included in the models the possible evolution of ^{17}O due to loss to space in order to see whether these measurements are consistent with various scenarios for atmospheric evolution.

Fractionation occurs as a result of nonthermal escape of oxygen to space, primarily because of the diffusive separation by mass of atmospheric species between the homopause (at about 125 km altitude) and the exobase (about 260 km). Species containing the lighter isotopes will be relatively more abundant at the exobase than those containing the heavier ones, so escape to space will preferentially remove the lighter isotopes. Simple models of this enrichment can be used to estimate the fractionation that occurs as oxygen is lost from the system; because atmospheric species can exchange or interact with nonatmospheric species, the amount of fractionation that results is a simple function of the fraction of the total oxygen reservoir that has been lost. The rate of loss of oxygen is sufficient to remove all of the oxygen from the atmosphere in 10^8 years; because the ratio of $^{18}O/^{16}O$ in CO_2 is near the value seen in silicates, there must be exchange with a large nonatmospheric reservoir. The physical evidence suggests that this reservoir is polar water ice, and that oxygen readily exchanges between CO_2 and H_2O.

These loss models have been modified to include loss of ^{17}O as well. The results are described in terms of $\Delta^{17}O$ ($=\delta^{17}O-0.52\delta^{18}O$); because most exchange processes change the value of $\delta^{17}O$ and $\delta^{18}O$ in a consistent pattern and along a line of slope 0.52, any departures of $\Delta^{17}O$ from 0 will be significant. Loss to space involves a nonlinear fractionation in $^{18}O/^{17}O/^{16}O$, so that there is no reason that the remaining oxygen should stay on this same mixing line; in fact, fractionation on Mars will initially be on a line of slope 0.55, moving it off the mixing line and resulting in $\Delta^{17}O > 0$. As oxygen is lost from the system, the models predict that $\Delta^{17}O$ will rise from 0 to a peak of almost 2‰ when about 1/3 of the oxygen in the system has been lost. As more oxygen is lost, $\Delta^{17}O$ decreases, crosses 0 when about half of the oxygen has been lost, and then continues to drop rapidly. The measurement of $\Delta^{17}O$ in the SNCs yields a value of $\Delta^{17}O=0.5$‰ relative to the oxygen in the silicates; this value is a lower limit due to possible contamination from terrestrial oxygen. At face value, the results suggest that the data are consistent with the loss of between about 5 and 50% of the oxygen in the system.

The present results should be viewed with caution because they do not include (i) possible differences in the escape efficiency of the different isotopes due to the energetics of the dissociative recombination escape mechanism, (ii) possible differences in the escape efficiency due to the altitude dependence of the solar wind pickup loss mechanism, or (iii) possible nonequilibrium isotopic exchange of oxygen between CO_2 and H_2O due to the photodissociation of each species and recombination from a combined oxygen reservoir.

These results are consistent with the previous $^{18}O/^{16}O$ data, which also suggest loss of less then half of the oxygen. They are still not consistent with the D/H in atmospheric H_2O, which suggests loss of >90% of the water in the system. The results can be reconciled by invoking a time-dependent exchange scenario due to the differing loss times for atmospheric water and CO_2. They cannot be reconciled with a model in which CO_2 buffers the oxygen and H_2O buffers the hydrogen; discrepancies occur due to (i) the probable lack of sufficient CO_2 in the regolith to adequately buffer the oxygen and (ii) the difficulty of its exchanging with atmospheric CO_2 due to the pore-blocking capability of stable ground ice.

It is important to recognize that escape to space provides a potentially important mechanism for producing non-zero values of $\Delta^{17}O$. The measured value, therefore, is completely consistent with the incorporation into the SNCs on Mars of water that had resided in the atmosphere and had evolved isotopically from its initial value at outgassing.

N92-28493

The Mars Water Cycle at Other Epochs: History of the Polar Caps and Layered Terrain.

Bruce M. Jakosky, Bradley G. Henderson, and Michael T. Mellon, Laboratory for Atmospheric and Space Physics, University of Colorado, Boulder CO 80309-0392, USA.

The atmospheric water cycle at the present epoch involves summertime sublimation of water from the north polar cap, transport of water through the atmosphere, and condensation on one or both winter CO_2 caps. Exchange with the regolith is important seasonally, but the water content of the atmosphere ap-

pears to be controlled by the polar caps. The net annual transport through the atmosphere, integrated over long timescales, must be the driving force behind the long-term evolution of the polar caps; clearly, this feeds back into the evolution of the layered terrain. We have investigated the behavior of the seasonal water cycle and the net integrated behavior at the pole for the last 10^7 years. Our model of the water cycle includes the solar input, CO_2 condensation and sublimation, and summertime water sublimation through the seasonal cycles, and incorporates the long-term variations in the orbital elements describing the martian orbit.

The calculated sublimation of water from the polar caps each season is based on the physical processes inferred to be operating at the present epoch, although there are clearly major assumptions that must be made to extrapolate to other epochs. Polar-cap temperature is calculated for each day throughout a Mars year using a standard thermal model, and sublimation of water is determined using Ingersoll's formulation. At obliquities lower than the present one, we assume that one cap retains its CO_2 covering year round and that the other one loses its covering during summer; this assumption is based on the rapid timescale with which CO_2 covering both caps will be transferred completely to one cap. For simplicity, we follow the present behavior and assume that the cap with summer nearest to aphelion is the exposed cap. At higher obliquities, we assume that both caps lose their CO_2 frost covering in summer, based on the paucity of residual CO_2 frost on the south polar cap at the present epoch. Finally, although there are clearly large uncertainties even at the present epoch, we assume that, at low obliquity, all water sublimed into the atmosphere in summer from one cap is lost to the other cap during the year; when both caps are uncovered in summer at high obliquities, we assume that the net transport is the difference in sublimation from the two caps. Although these assumptions may not be valid, they give us a basis for discussing the long-term evolution of the caps.

Net long-term transport results because of the difference in elevation of the two caps; this is the one property that we have not taken to be the same for both caps. Because the south cap is higher than the north cap, the CO_2 partial pressure will be lower over it, resulting in preference for CO_2 frost deposits at the north pole. While this may not be the case for any single year (witness the present epoch), this effect will cause a net long-term preference for transport of water to the north cap when averaged over all orbital elements. This behavior may explain the difference in the sizes of the two residual caps: As water is transported north due to this imbalance, the south cap shrinks and the north cap grows. This causes the sublimation integrated over the cap area to increase in the north and decrease in the south until a stable steady-state point is reached. At this point, the product of average sublimation rate times area will be the same for both caps.

We can also look at the departures from the mean behavior of the amount of water ice residing on each cap. Although up to tens of centimeters of ice can sublime from the surface of one cap during each summer at the highest obliquities, the average or integrated effects are generally smaller than this. The largest excursion of the amount of ice at one pole is less than about 1 km at the south cap, and most excursions are much smaller than this. The result is that, at least on timescales of 10^7 years, only about 1 km of ice shifts between the two caps; this translates to less than 1 km at the north cap due to its larger area. This result may help us to understand the apparent discrepancy between the age of the south-polar layered deposits as determined using crater counts by Plaut et al. (10^7–10^8 years) and the timescale for creating layers in the layered deposits inferred from the timescale for changing the orbital elements (10^5–10^6 years). That is, the individual layers can still be formed on the shorter timescales; as it is much of the same water moving back and forth between the caps, the net accumulation of water ice at one pole is less than 1 km in 10^7 years and longer.

The present results are extremely model dependent in terms of the specific quantitative behavior of the water cycle and of the ice abundance at each pole. Further, the quantitative aspects of the model do not agree exactly with the observations at the pole. Despite this, we have not varied parameters in our model in order to try to better match the data. The utility of such an exercise is precluded by uncertainties in the behavior of various processes at other epochs; these uncertainties include (i) the possible enhancement of dust storms at high obliquity, their inhibition at low obliquity, and their quantitative effects on the CO_2 and H_2O cycles, (ii) the possible dependence of CO_2 albedo on insolation as suggested by Paige, (iii) the uncertainties in the albedo of the water-ice residual cap(s) at other epochs, (iv) the inability to determine which cap should retain a CO_2-frost covering throughout the year (even at the present epoch), (v) the possible inhibition of sublimation of water ice by the build-up of a layer of dust or dirt at the ice surface, and (vi) the large uncertainty in the history of the obliquity even as recently as 10^7 years. However, the general nature of the results is not as model dependent. They clearly show (i) a preferred long-term presence of CO_2 frost at the north despite its current preference for the south, and (ii) the cyclical exchange of relatively small amounts of water between the caps on timescales up to 10^7 years. These trends are exactly those we expect based on our understanding of the physics behind the current seasonal cycles..

Mars Global Reference Atmosphere Model (Mars-GRAM).

C. G. Justus, Georgia Institute of Technology, School of Geophysical Science, Atlanta GA 30332, USA and Bonnie F. James, NASA Marshall Space Flight Center, Huntsville AL 35812, USA.

Mars-GRAM is an empirical model that parameterizes the temperature, pressure, density, and wind structure of the martian atmosphere from the surface through thermospheric altitudes [1,2]. In the lower atmosphere of Mars (up to 75 km) the model is built around parameterizations of height, latitudinal, longitudinal, and seasonal variations of temperature determined from a survey of published measurements from the Mariner and Viking programs (Fig. 1) [3]. Pressure and density are inferred from the temperature by making use of the hydrostatic and perfect gas laws relationships. For the upper atmosphere (above 120 km), the thermospheric model of Stewart [4] is used. A hydrostatic interpolation routine is used to insure a smooth transition from the lower portion of the model to the Stewart thermospheric model. Mars-GRAM includes parameterizations to simulate the effects of seasonal variation, diurnal variation, effects due to the orbital position of Mars, effects of the large seasonal variation in surface atmospheric pressure because of differential condensation/sublimation of the CO_2 atmosphere in the polar caps, effects of martian atmosphere mountain wave perturbations on the magnitude of the expected density perturbations, and local-scale to global-scale dust storm effects (Fig. 2). The thermospheric

model includes a parameterization for the effects of solar activity, measured by the 10.7-cm solar radio flux. Winds are computed by an areostrophic (thermal wind) approximation, with the inclusion of the effects of molecular viscosity, which, because of the low atmospheric densities, can be very important at high altitudes. The mountain wave perturbation model also includes a new damping approximation due to the effects of molecular viscosity. The Zurek wave perturbation model [5] has also been incorporated to simulate the effects of tidal perturbations (Fig. 3).

The Mars-GRAM has numerous applications as a "poor man's global circulation model." For example, the computation of all of the data necessary to describe the complete seasonal variations at the surface and all altitudes takes at most a few minutes on a PC, whereas comparable data results using a 3-D global circulation model would take many hours of computation on a mainframe. There are many specific scientific applications as well. One of these is Mars-GRAM's ability to provide a realistic geographically and seasonally dependent background of temperatures and winds for studies of tides and the atmospheric propagation of other wave disturbances. Another application would be in providing realistic "first guess" profiles for the inversion processing for temperature retrievals from temperature sounders on upcoming Mars missions.

Continued analysis of additional observational data from the Mariner and Viking programs provided through PANDA and other on-line systems, analysis of new results from global circulation models, and analysis of new data expected from Mars '94 and the Mars Observer programs, will all provide a basis for continued improvements in the Mars-GRAM.

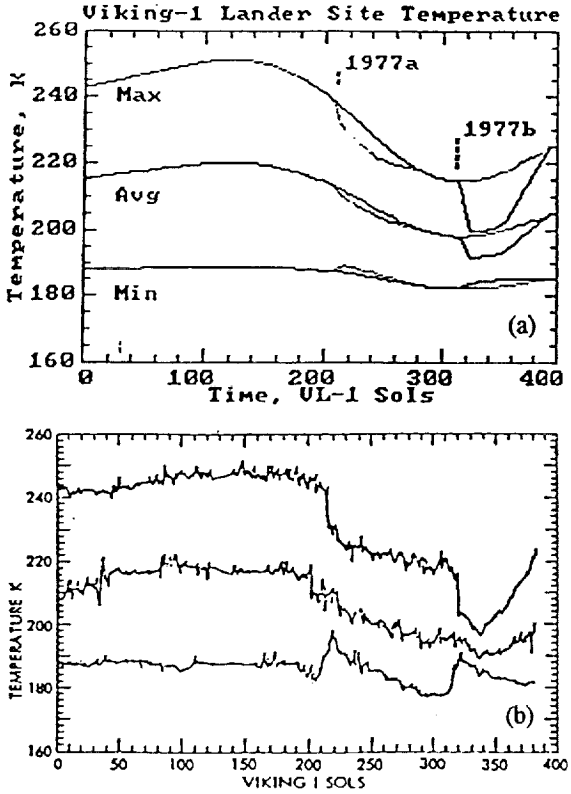

Fig. 1. The seasonal variation of the daily maximum, mean, and minimum temperature at the Viking Lander site, (a) computed by Mars-GRAM, and (b) as reported by Ryan and Henry [3].

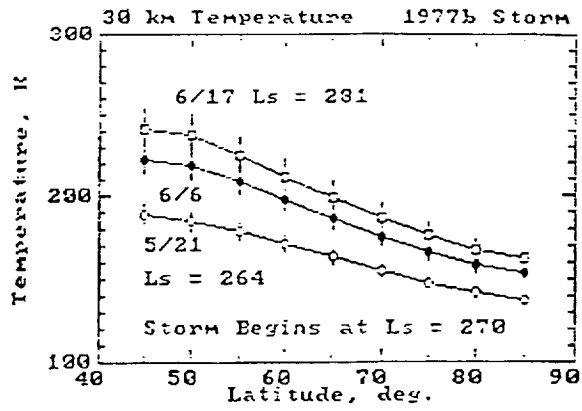

Fig. 2. The progression of simulated dust-storm effect on daily average, maximum, and minimum temperature vs. latitude for the 1977b storm.

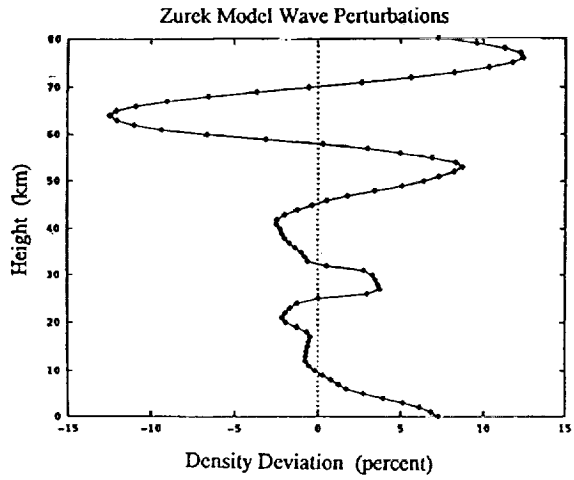

Fig. 3. A sample evaluation of the Zurek density wave perturbation model (based on temperature perturbation parameters in [5]). Location and time corresponds to that of the Viking 1 Lander entry.

References: [1] Justus C. G. (1991) *J. Spacecraft and Rockets, 28*, 216–221. [2] Justus C. G. (1989) *NASA Technical Report*, 10/8/89. [3] Ryan J. A. and Henry R. M. (1979) *JGR*, 2821–2829. [4] Stewart A. I. F. (1987) *JPL Report NQ-802429*, 3/26/87. [5] Pitts D. E. et al. (1988) *JSC Technical Report #24455.*

N92-28495

A Reduced Atmosphere for Early Mars? J. F. Kasting, Department of Geosciences, 211 Deike, Penn State University, University Park PA 16802, USA.

One-dimensional, radiative-convective climate calculations indicate that the old model [1] of a warm, dense, CO_2 atmosphere on early Mars is no longer viable. The magnitude of the greenhouse effect in a CO_2/H_2O atmosphere is limited by con-

densation of CO_2 clouds; this phenomenon is not important for Mars today, but has a pronounced cooling effect at the low solar luminosities thought to apply during early solar system history [2]. The failure of this model indicates one of four things: Either i) the new climate calculations are incorrect, ii) current solar evolution models are incorrect, iii) the idea that early Mars was warm and wet is incorrect, or iv) the atmosphere of early Mars contained other greenhouse gases (or particles) in addition to CO_2 and H_2O.

Of these explanations, the most plausible is number (iv). The idea is not new: high concentrations of ammonia were postulated by Sagan and Mullen [3] as the solution to the faint young Sun problem on both early Earth and early Mars. Subsequent calculations, however, indicated that ammonia would have been rapidly converted to N_2 and H_2 by photolysis [4,5]. Furthermore, no obvious source for ammonia could be identified, since modern terrestrial volcanic gases are sufficiently oxidized that most of the nitrogen should be in the form of N_2 [6].

Here, I consider whether volcanic gases released from early Earth and, by analogy, early Mars could have been more reduced than modern volcanic gases. New evidence from sulfide inclusions in diamonds [7] indicates that the Archean mantle was substantially more reduced than today. At least parts of it had an oxygen fugacity, f_{O2}, close to the iron-wüstite (IW) buffer, about four log units lower than than today's mantle f_{O2}, which is close to the quartz-fayalitemagnetite (QFM) buffer. The argument for a reduced Archean mantle is strengthened by Murthy's observation [8] that mantle siderophile abundances are consistent with equilibrium partitioning at high temperatures following the Moon-forming impact. This implies that the mantle was originally at equilibrium between molten iron and molten silicates, so its oxygen fugacity should have been close to IW. The transition from IW to QFM could have been caused by recycling of H_2O and CO_2 through the mantle, followed by release of H_2 and CO from volcanoes. If Earth and Mars started out with reduced mantles, CH_4 and NH_3 should have been present in volcanic gases at about the 0.1% level [6]. This finite source, combined with UV shielding by hydrocarbon particles formed from methane photolysis, could have produced enough CH_4 and NH_3 to augment the greenhouse effect and produce a warm climate on early Mars.

References: [1] Pollack J. B. et al. (1987) *Icarus, 71*, 203–224. [2] Kasting J. F. (1991) *Icarus, 94*, 1–13. [3] Sagan C. and Mullen G. (1972) *Science, 177*, 52–56. [4] Kuhn W. R. and Atreya S. K. (1979) *Icarus, 37*, 207–213. [5] Kasting J. F. (1982) *JGR, 87*, 3091–3098. [6] Holland H. D. (1984) *The Chemical Evolution of the Atmosphere and Oceans*, p. 50, Princeton Univ. [7] Eggler D. et al., manuscript in preparation. [8] Murthy V. R. (1991) *Science, 253*, 303–306.

N92-28496

Influences of CO_2 Sublimation/Condensation Processes on the Long-Term Evolution of the Martian Atmosphere. K. Kossacki and J. Leliwa-Kopystynski, Institute of Geophysics of Warsaw University, ul. Pasteura 7, 02-093 Warszawa, Poland.

Outgassing models suggest that at least 140 mbar and possibly as much as 3000 mbar of CO_2 have been placed in the martian atmosphere over geological time (Kahn, 1985). On the other hand, it is known that the present pressure on the martian surface varies seasonally around a value as low as a few millibars, so it is very interesting to study the evolution of CO_2 content in the atmosphere.

In this work the accumulation process of frozen CO_2 within the martian regolith is analyzed. The boundary conditions are taken to be the periodically variable temperature at the Mars surface and the constant heat flux at the bottom of the regolith layer, some hundred meters thick. The mean value of temperature as well as its amplitude are assumed to be dependent on latitude and could be variable with the geological time scale. The flux of gaseous CO_2 within the regolith is controlled by the mechanism of gas transport through the porous medium. An appropriate initial geometry of distribution of pores is assumed. The porosity and flux change due to condensation/sublimation processes. The equations of heat and mass transfer are solved numerically for a given latitude. Next, the local (over the parallel of latitude belt) annual balance of CO_2 is calculated. The procedure is repeated over the whole martian surface and next the total annual net flux is calculated.

N92-28497

CO_2 and Clathrate as Past Erosive Agents on Mars. R. St. J. Lambert, Department of Geology, University of Alberta, Edmonton, Alta, T6G2E3, Canada and V. E. Chamberlain, Department of Geology, University of Idaho, Moscow ID 83843, USA.

The debate on the history of the martian atmosphere continues without resolution. Much hinges on a satisfactory solution to the problem of what liquid was responsible for the extensive development of canyons, channels, fretted terrain, and similar features. The 1960s and 1970s saw much debate about the roles of various fluids, namely water or brine, liquid CO_2, or H_2O sources in CO_2 clathrate ("CC"), or magma. The last has long been discounted, CC has largely been ignored, and the most recent look at CO_2 was by ourselves [1], utilizing the phase diagrams for the CO_2-H_2O system [2–4]. We argued that the canyons, primarily of tectonic origin, were given their detailed shape because of the presence of liquid CO_2 trapped beneath CC or CO_2 permafrost. Faulting or fissuring was a possible trigger for the release of the liquid, which would automatically boil on reduction of pressure, thus causing slumping and foundering of the terrain. Pit-chains were also explained this way. This is a uniformitarian model, in that present-day martian temperatures (specifically near 210°K) are suitable for this process, so that no special conditions are required in the past. The chaotic terrain/braided channel regions were considered to be a consequence of a similar process, but in this case, magmatic heat and a denser atmosphere had to be invoked in order to explain the massive flooding.

A problem with this theory was the requirement of too great a depth (330 m) for the liquefaction to be effective as an erosive or destructive agent. This parameter is a function of the pressure on the volatile. Its value can be made more reasonable if higher pressures, approaching load pressure, are chosen for the CO_2 in place of the 0.2×P (total) that was originally used. Then liquid CO_2 could be present at 60 m depth and 220°K for the surface temperature, or (for example) at 200 m and about 250°K. The former does not require much of a greenhouse effect, and we do not see any reason why higher pressures could not have existed at shallow depth. On Earth, overpressured fluids are common even where the volatile has a negligible partial pressure at the surface.

Another problem is the lack of a sink for the former atmospheric CO_2. This problem has only been discussed in general terms. Three common minerals offer potential as sinks: $CaCO_3$, calcite; $MgCO_3$, magnesite; and $FeCO_3$, siderite. On Earth, $CaCO_3$ is the first mineral to precipitate from sea-water-type brines undergoing evaporation. $MgCO_3$ is readily formed at temperatures above about 300°C at any typical crustal or upper mantle pressure (by the reaction of CO_2 with Fe-Mg silicates, especially serpentine). The mineral of most significance, though, is siderite. It forms from magnetite or hematite, or by direct precipitation, in any sedimentary environment with adequate Fe, relatively high concentrations of CO_2 in solution (e.g., molar), pH 7–8, and Eh at a reducing (C-bearing) level. It is extremely difficult to imagine a martian subsurface that could not have met these conditions in the regolith at some past time. Therefore siderite is likely to be common in the deeper, unoxidized martian regolith, too deep to have been sampled by the Viking landers.

It is the very conditions that we are discussing, a cool subsurface containing some liquid CO_2, that would seem to ensure the reaction of magmatic or secondary iron oxides to siderite. As basalts can commonly have 5% iron oxides, an atmosphere of CO_2 could slowly but surely be converted to $FeCO_3$. We note that the warmer the surface, the deeper is the zone of liquid CO_2. Thus as the surface cooled due to the removal of greenhouse gases to depth, the top of the zone of reactive liquid CO_2 would migrate upward. If this had been occurring at a time of basic volcanism, it would cause a kind of vicious circle, which would progressively strip the atmosphere of CO_2. This theory of the cause of the loss of CO_2 is in accord with the known history of Mars: the major erosion precedes or accompanies the cratered northern volcanic plains, the growth of which would trap the CO_2 in siderite.

The role of CC is rather more simple. Its presence at the surface today can be considered unlikely, from reaction rate and other considerations. At depth the situation is entirely different. At any temperature above 213°K and at moderate depths, <500 m or so, liquid CO_2 may be or have been present, and it should react quickly with solid H_2O to produce CC. The upper temperature stability limit of CC has a positive slope in PT space, such that solid CC always physically underlies combinations of CO_2 and H_2O. If excess CO_2 is present, CC can overlie liquid CO_2 at 270°C). If excess H_2O is present, CC can overlie liquid H_2O at >~270°K, but only at >~150 m depth. The simplest role of CC is therefore as a trap, to keep liquids below it at lithostatic pressure. Its other role is as a reservoir of H_2O, stored ready to be decompressed and converted to fluid [3] or warmed by magmas, and fluidized [1].

The existence of past greenhouse effects is also relevant. Arguments are currently finely balanced over the question of whether any significant warming could have occurred on Mars. If it was warmer in the past, then the latitude of the zone of potential erosion by CO_2 moves towards the poles, maintaining the likelihood of our preferred method of erosion. However, it requires warming by some 40°C before liquid H_2O is possible on a large scale at the surface, particularly at its present low partial pressure. As the greenhouse would most likely be caused by CO_2, any argument in its favor also increases the likelihood of erosion by liquid CO_2, and increases the chance of the creation of large volumes of CC. The greenhouse would not necessarily, though, create the required conditions for erosion by rain or surface water.

References: [1] Lambert R. St. J. and Chamberlain V. E. (1978) *Icarus, 34*, 568–580. [2] Miller S. L. and Smythe W. D. (1970) *Science, 176*, 531–533. [3] Milton D. J. (1974) *Science, 183*, 654–656. [4] Mutch T. C. et al. (1976) *The Geology of Mars*, Princeton Univ.

N92-28498

History of Oxygen and Carbon Escape from the Martian Atmosphere. J. G. Luhmann[1], M. H. G. Zhang[2], R. E. Johnson[3], S. W. Bougher[4], and A. F. Nagy[5], [1]Institute of Geophysics and Planetary Physics, University of California, Los Angeles CA 90024, USA, [2]Space Research Institute, Austrian Academy of Sciences, Graz, Austria, [3]University of Virginia, Charlottesville VA, USA, [4]University of Arizona, Tucson AZ, USA, [5]University of Michigan, Ann Arbor MI, USA.

A fraction of the oxygen in the martian atmosphere continually escapes to space because dissociative recombination of the O_2^+ ions in the ionosphere can impart sufficient energy to the product O atoms. In addition, ionization of the extended atomic oxygen corona resulting from the above process adds to escape since the solar wind can carry away O^+ ions born above a few hundred km altitude. A further by-product of this ion-pickup by the solar wind is an additional population of escaping oxygen atoms that are sputtered from the atmosphere near the exobase by pickup ions that are on reentry rather than escaping trajectories. This sputtering process can also remove carbon in the form of intact or dissociated CO_2 since all atoms and molecules in the "target" gas are subject to the collisional energy transfer that characterizes sputtering [1].

We have estimated the present rates of escape of oxygen and carbon due to these mechanisms, as well as the rates at several epochs in the history of the solar system. For this purpose we calculated the expected attributes of the upper atmosphere, ionosphere, and exosphere (escaping + trapped components) expected under conditions of 1×, 3× and 6× the present solar EUV flux, the corresponding pickup ion fluxes based on a model of early solar wind properties, and the sputtered fluxes of O and CO_2 resulting from the reentering pickup ions. We find the following loss rates for these epochs:

Epoch (solar emission in terms of the present EUV flux)	Exospheric O escape (atom/s)	Pickup O^+ ion escape (ion/s)	Sputtered O escape (atom/s)	Sputtered CO_2 escape (molecule/s)
1 EUV	8×10^{25}	6×10^{24}	3×10^{23}	3×10^{23}
3 EUV	5×10^{26}	4×10^{26}	3×10^{26}	6×10^{25}
6 EUV	1×10^{27}	3×10^{27}	3×10^{27}	3×10^{26}

Some models of the early sun (e.g., [2]) suggest that the 6 EUV case corresponds to a solar system age of ~1 Gyr, while 3 EUV corresponds to ~2 Gyr age. By integrating these loss rates up to the present, presuming a linear interpolation can be used for intervening periods, we estimate cumulative losses to date of 2×10^{44} atoms for oxygen and 6×10^{42} atoms for carbon by escape to space. The oxygen loss is equivalent to that in 50 m of water, while the lost carbon could supply a 0.4 bar atmosphere. A missing piece of this puzzle that remains to be included is the loss of carbon from dissociative recombination of CO^+ during the

high EUV conditions (current estimates are comparable to the 1-EUV sputtering rate [3]). These losses are to be considered in addition to any early losses (age ≤ 1 Gyr) due to hydrodynamic escape and impact erosion.

References: [1] Johnson R. E. (1990) *Energetic Charged-Particle Interactions with Atmospheres and Surfaces*, Springer-Verlag Berlin, pp. 174–180. [2] Zahnle K. J. and Walker J. C. G. (1982) *Rev. Geophys., 20*, 280. [3] McElroy M. B. (1972) *Science, 175*, 443.

Using the Historical Record to Determine Dust Sources. L. J. Martin, Lowell Observatory, 1400 West Mars Hill Road, Flagstaff AZ 86001, USA.

We have recently completed a study of virtually all reported dust activity noted in contemporary and historical records of Mars observations [1]. This study included the compilation of maps showing the locations of these events to the degree that they could be determined. Whenever possible, regional (major) storms were individually mapped, as well as on a composite map. Areas of local events were shown only on a composite map. The four mappable planet-encircling storms were each given separate treatment on maps that portray their development around the planet.

Although dust activity can occur at any location (and in 1971 at all locations), some areas are more prone to be active than others. The Hellas basin seems to be the most frequently active dust area, regardless of whether that activity is local, regional, or planet-encircling. Some observers and researchers may even accept this as the "normal" condition for that area, although Hellas is not even a bright entity during some martian apparitions. Nevertheless, no other area on Mars can be considered as such a prime candidate for a dust source as Hellas. The southern half of Hellas is also the site of polar hood and seasonal cap activity during southern winter and early southern spring. These polar phenomena must play a role in this Hellas dust activity, but the nature and degree of this role are still uncertain.

The Argyre basin is another site of frequent dust activity that is also partially within the boundaries of seasonal polar activity. This smaller basin is usually less bright than Hellas and often darkens to become invisible on albedo maps. The seasonality of these albedo changes needs further study. Ranking near Argyre in dust activity is the Noachis Terra. This area is generally light but not bright. It covers most of the area between the above basins at similar latitudes, again including polar activity. Although Noachis may be less likely to be the site of initial clouds, growing major storms may "feed" on dust sources they find there.

Dust clouds are most frequently observed in light areas but are also often seen in dark areas. In either case there is little concern for observational effects created by background albedo except when observers describe long-lasting, stationary hazes, which could be questionable as atmospheric features. Dark areas that are repeated sites of dust activity are Syrtis Major, Solis Lacus, and Hellespontis.

The initial clouds for some regional storms and all those that can be identified for planet-encircling storms have been in darkish areas. The 1956 and 1971 storms began in Hellespontis. The 1973 storm began at first in Solis Lacus and later in Sinus Meridiani. The 1924 storm (see figure) was not well observed, coming very late in the apparition. The most important observations were by whole-disk polarimetry. Probably no photographs exist; however, an early visual observation placed it crossing over Hellespontis between Hellas and Noachis, making it very reminiscent of observations of more recent planet-encircling storms. The storm in 1924 is the only unimaged storm that we put in the encircling category, except for the 1982 storm observed by Viking Lander I. It is suggested that certain dark areas must also be able to act as dust sources for initial clouds of larger storms, although these storms quickly move to lighter areas as they expand.

Reference: [1] Martin L. J. and Zurek R. W. (1992) *JGR Planets*, submitted.

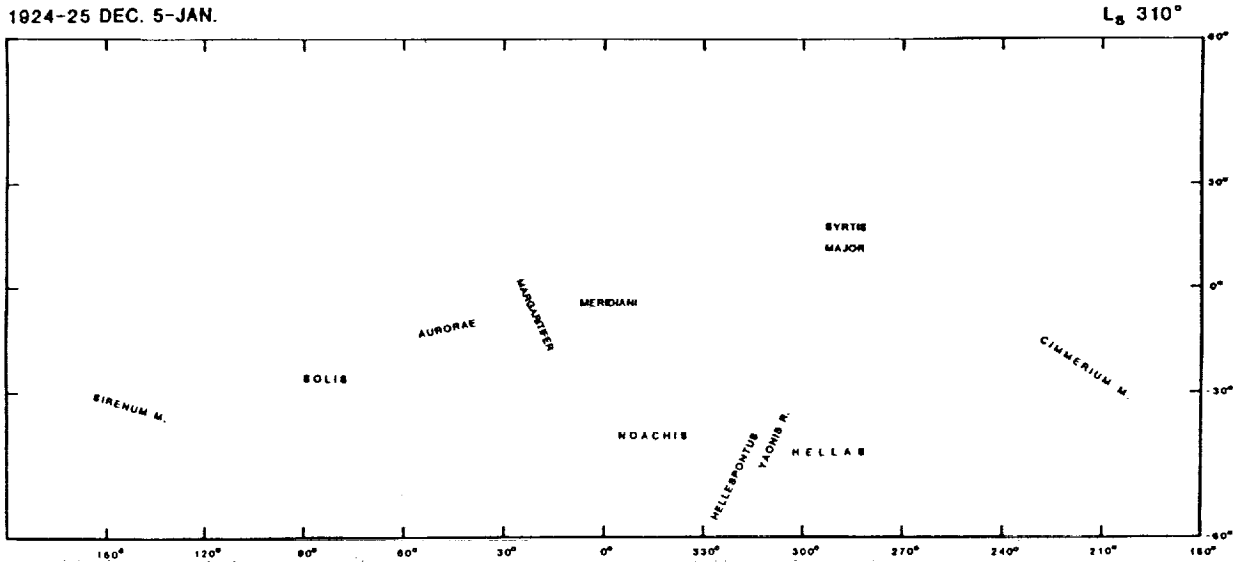

N92-28500

Liquid Water Habitats on Early Mars. Christopher P. McKay and Wanda L. Davis, Space Science Division, NASA Ames Research Center, Moffett Field CA 94035, USA.

Although the Viking results may indicate that Mars has no life today, the possibility exists that Mars may hold the best record of the events that led to the origin of life. There is direct geomorphological evidence that in the past Mars had large amounts of liquid water on its surface. Atmospheric models would suggest that this early period of hydrological activity was due to the presence of a thick atmosphere and the resulting warmer temperatures [1]. From a biological perspective the existence of liquid water *by itself* motivates the question of the origin of life on Mars. From studies of the Earth's earliest biosphere, we know that by 3.5 Gyr ago life had originated on Earth and reached a fair degree of biological sophistication. Surface activity and erosion on Earth make it difficult to trace the history of life before the 3.5-Gyr timeframe. If Mars did maintain a clement environment for longer than it took for life to originate on Earth, then the question of the origin of life on Mars follows naturally [2,3].

Based upon simple models of the evolution of the martian climate [1,4], we divide the history of liquid water habitats on the martian surface into four epochs based upon the atmospheric temperature and pressure [5]. In Epoch I, during which a primordial CO_2 atmosphere was actively maintained by impact and volcanic recycling, we presume the mean annual temperature to have been above freezing, the pressure to have exceeded one atmosphere, and liquid water to have been widespread. Under such conditions, similar to early Earth, life could have arisen and become abundant. After this initial period of recycling, atmospheric CO_2 was irreversibly lost due to carbonate formation and the pressure and temperature declined. In Epoch II, the mean annual temperature fell below freezing but peak temperatures would have exceeded freezing. Ice-covered lakes, similar to those in the McMurdo Dry Valleys of Antarctica, could have provided a habitat for life. In Epoch III, the mean and peak temperatures were below freezing and there would have been only transient liquid water. Microbial ecosystems living in endolithic rock "greenhouses" could have continued to survive [6,7]. Finally, in Epoch IV, the pressure dropped to near the triple-point pressure of water and liquid water could no longer have existed on the surface and life on the surface would have become extinct.

References: [1] Pollack J. B. et al. (1987) *Icarus, 71*, 203–224. [2] McKay C. P. (1986) *Adv. Space Res., 6*, 269–285. [3] McKay C. P. and Stoker C. R. (1989) *Rev. Geophys. Space Phys., 27*, 189–214. [4] McKay C. P. and Davis W. L. (1991) *Icarus, 90*, 214–221. [5] McKay C. P. et al. (1992) *Adv. Space Res., 12*, 231–238. [6] Friedmann E. I. (1982) *Science, 215*, 1045–1053. [7] Friedmann E. I. et al. (1987) *Polar Biology, 7*, 273–287.

N92-28501

Martian Atmospheric Chemistry During the Time of Low Water Abundance. Hari Nair[1], Mark Allen[1], Yuk L. Yung[1], and R. Todd Clancy[2], [1]Division of Geological and Planetary Sciences 170-25, California Institute of Technology, Pasadena CA 91125, USA, [2]Laboratory for Atmospheric and Space Physics, University of Colorado, Boulder CO 80309-0392, USA.

The importance of odd hydrogen (or HO_x) radicals in the catalytic recombination of carbon monoxide and oxygen in the martian atmosphere has been known for many years [1,2]. The inclusion of recent chemical kinetics data, specifically temperature-dependent CO_2 absorption cross sections [3], into our one dimensional photochemical model shows that HO_x is too efficient in this regard. The absorption cross sections of CO_2 are smaller than previously assumed; this leads to a reduction in the photolysis rate of CO_2 while the photolysis rate of H_2O has increased [4]. As a consequence the predicted mixing ratio of CO in our models is substantially less than the observed value of 6.5×10^{-4}.

Simultaneous measurements of water [5], ozone [6], and carbon monoxide [6] have been recently obtained in the martian atmosphere in early December 1990 (L_s for Mars was 344°). The global average water abundance was ~3 μm, with a mixing ratio ranging from 70 ppm at low latitudes to below 20 ppm at high latitudes.

If such low water abundances are typical for the martian atmosphere over long timescales, the efficiency of the HO_x catalytic cycle may be severely curbed. Indeed, Shimazaki [7] pointed out that a "typical" water abundance of ~10 μm produced a model CO abundance much lower than observed, while a lower H_2O abundance of ~1.4 μm produced a CO abundance consistent with observations.

TABLE 1. Epochs of liquid water habitats on Mars.

Epoch number	Possible duration Gyr ago	Thermodynamic conditions	State of liquid water	Biological analogs
I	4.2–3.8	$P \geq 5$ atms $T > 0$°C	liquid water abundant	origin of life possible
II	3.8–3.1	$T < 0$°C $T_{peak} > 0$°C	ice-covered lakes	microbial mats in lakes
III	3.1–1.5	$T_{peak} < 0$°C $P >> 6.1$ mb	liquid water in porous rocks	life inside rocks
IV	1.5–present	$P \equiv 6.1$ mb	pressure at triple point, no liquid water	no life on the martian surface

The seasonally varying concentration of ozone is a valuable indicator of the abundance of HO_x, as it is typically destroyed by reactions such as $H + O_3 \rightarrow OH + O_2$. Its lifetime is on the order of tens of minutes, so that it adjusts virtually instantaneously to variations in the water abundance. Ozone amounts at the equator were measured to be <1 μm, which is smaller than what our photochemical model indicates.

Our aim is to examine the ability of gas-phase chemistry to control the composition of the martian atmosphere. The expected results of lowering the abundance of HO_x are higher mixing ratios for both CO and O_3. Differences between models and observations may require the inclusion of additional gas-phase mechanisms, and possibly heterogeneous chemistry, for example, to curtail the HO_x cycle as suggested by Anbar et al. (1992) [8].

References: [1] McElroy M. B. and Donahue T. M. (1972) *Science*, 986–988. [2] Parkinson T. M. and Hunten D. M. (1972) *J. Atmos. Sci.*, 1380–1390. [3] Lewis B. R. and Carver J. H. (1983) *J. Quant. Spectrosc. Radiat. Transf.*, 297–309. [4] Anbar A. D. and Allen M. (1992) *JGR*, in press. [5] Clancy R. T. et al. (1992) *Icarus*, in preparation. [6] R. T. Clancy, personal communication. [7] Shimazaki T. (1989) *J. Geomag. Geoelectr.*, 273–301. [8] Anbar A. D. et al. (1992) *JGR*, in press.

N92-28502

The Early Martian Atmosphere. Robert O. Pepin, School of Physics and Astronomy, University of Minnesota, Minneapolis MN 55455, USA.

Atmospheric noble gases on Mars, Earth, and Venus are severely and variably depleted with respect to solar abundances, and are characterized by isotopic signatures that differ from planet to planet and from meteoritic and inferred solar compositions. Earlier theories based on simple accretion of meteoritic veneers as planetary volatile sources [1] are unable to replicate these distributions, and so attention is now focusing on evolutionary processes that can fractionate both elements and isotopes, operating either on the early planets themselves [2–6] or in large preplanetary planetesimals [7]. Hydrodynamic escape of hydrogen-rich primary atmospheres and outgassed volatiles from the terrestrial planets can account for most of the known details of noble gas distributions in their present-day atmospheres [5]. In a current model of the process [5,6] each planet acquires two isotopically solar volatile reservoirs during accretion, one adsorbed from nebular gases onto planetary core materials and the other coaccreted as a primary atmosphere degassed from impacting planetesimals. Subsequent fractionating losses of primary and outgassed species from Mars and Venus are driven by intense extreme-ultraviolet (EUV) radiation, declining with time, from the young evolving Sun. On Earth it appears that atmospheric escape driven by energy deposited in a giant Moon-forming impact could have been responsible for generating contemporary distributions of Xe, Kr, and Ar [6]. In this giant impact (GI) model, the planets were shielded from solar EUV radiation by collisional dust and remnant nebular gas for ≈100 m.y. or longer, by which time its intensity had declined to the point where only terrestrial Ne and lighter species were affected by EUV-driven escape. However, the relatively weak EUV flux (60× the present solar level) needed to drive Ne-only loss from Earth would still have been strong enough to enable hydrodynamic outflow of Kr and lighter gases from Venus, and all noble gases from the much smaller Mars.

Noble Gases on Mars: This escape model yields the results shown in Fig. 1 for evolution of primary and outgassed noble gases on Mars. EUV-driven escape of the hydrogen-rich (~50 bars H_2) primary atmosphere is assumed to begin at a solar age of 100 m.y. Two primary noble gas, CO_2 and N_2 components are mixed with the H_2—a "solar-like" component with solar isotopic compositions, and elemental abundances derived from model results for Venus' primary atmosphere [6] (assuming that an icy, Halley-like planetesimal source accreted by Venus would also have contributed to Mars); and a carbonaceous chondrite (CI) component inferred from strong isotopic evidence that martian Xe is predominantly massfractionated CI Xe and from bulk chemical modeling [5,8]. The "solar"/CI mixing ratio for Xe is ~0.03. The first escape stage (EUV-1) proceeds for 25 m.y., until halted by H_2 depletion and increasing atmospheric molecular weight. This episode fractionates all atmospheric noble gases as shown in Fig. 1, with abundance depletions given by the italicized numbers (all in units of 10^{-16} g/g-Mars). Primary Xe is fractionated to the composition represented by the horizontal line

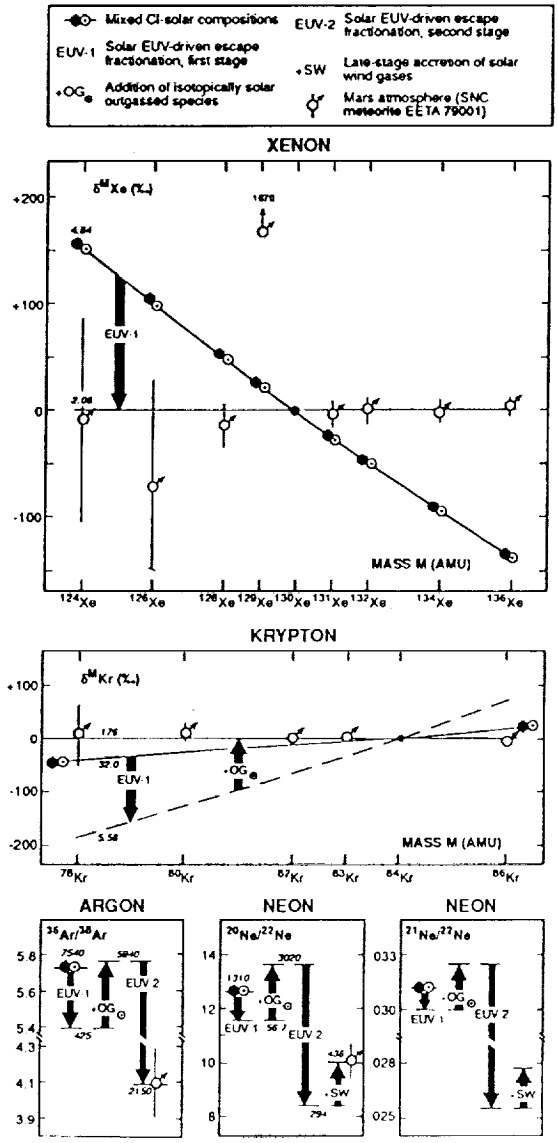

Fig. 1.

N92-28503

Astronomical Variation Experiments with a Mars General Circulation Model. J. B. Pollack, R. M. Haberle, J. R. Murphy, J. Schaeffer, and H. Lee, NASA Ames Research Center, Moffett Field CA 94035-1000, USA.

On time scales of a hundred thousand to a million years, the eccentricity of Mars orbit varies in a quasi-periodic manner between extremes as large as 0.14 and as small as 0 and the tilt of its axis of rotation with respect to the orbit normal also varies quasi-periodically between extremes as large as 35° and as small as 15°. In addition, the orientation of the axis precesses on comparable time scales. These astronomical variations are much more extreme than those experienced by the Earth. These variations are thought to have strongly modulated the seasonal cycles of dust, carbon dioxide, and water. One manifestation of the induced quasiperiodic climate changes may be the layered terrain of the polar regions, with individual layers perhaps recording variations in the absolute and/or relative deposition rates of dust and water in the polar regions, most likely in association with the winter time deposition of carbon dioxide ice.

In an attempt to understand the manner in which atmospheric temperatures and winds respond to the astronomical forcings, we have initiated a series of numerical experiments with the NASA/Ames general circulation model of the Martian atmosphere. For example, we have carried out runs close to summer solstice in the southern hemisphere for times at which the eccentricity had its largest and smallest possible values. Comparisons of these experiments with one another and with a run at a similar seasonal date for the current eccentricity indicate that substantial changes in surface wind stresses occur among the various cases. Surface wind stresses are largest at times of largest eccentricity when the planet is close to perihelion, implying a greater dust lifting capability at these times.

We are also examining the possible formation of perennial carbon dioxide ice caps at one or both poles at times of low obliquity. The initial experiments are being conducted with a 2D model to permit us to run the model for several Martian years, and thereby enable us to reach steady state conditions.

N92-28504

Regional Climatic Effects of Atmospheric SO_2 on Mars. S. E. Postawko[1] and F. P. Fanale[2], [1]School of Meteorology, University of Oklahoma, Norman OK 73019, USA, [2]Planetary Geosciences, University of Hawaii, Honolulu HI 96822, USA.

The conditions under which the valley networks on Mars may have formed remains controversial. The magnitude of an atmospheric greenhouse effect by an early massive CO_2 atmosphere has recently been questioned by Kasting [1]. Recent calculations indicate that if solar luminosity were less than about 86% of its current value, formation of CO_2 clouds in the martian atmosphere would depress the atmospheric lapse rate and reduce the magnitude of surface warming [1].

There is certainly a possibility that standard solar models, which predict that early solar luminosity was 25–40% less than at present [e.g., 2,3], may be incorrect and the early Sun may have been much brighter than previously assumed. Recent calculations by Graedel et al. [4] indicate that the weak early Sun paradox may be solved by assuming a 10% mass loss of the young Sun. Graedel et al. use this mass loss to provide a solution to the problem of "missing" solar lithium, as well as to suggest that above freezing surface temperatures on early Earth and Mars may have been possible without invoking extremely high CO_2 concentrations. The problem with this scenario is that it may, in fact, keep early Earth *too* warm [1]. Further calculations and observations are necessary before abandoning the standard solar model.

Other greenhouse gases, such as ammonia and methane, have been suggested as possibilities to keeping surface temperatures above freezing on early Mars [e.g., 5,6,1]. However, a way must be found to provide a steady source of these gases in light of rapid photodissociation [7], or to protect them from photodissociation. Greenhouse warming by minor gases such as HCN and N_2O has also been explored [8].

The difficulties presented by an enhanced atmospheric greenhouse effect have led to suggestions that higher early heat flow on Mars kept near-surface temperatures high enough to mobilize groundwater. However, in the absence of precipitation it is difficult to explain how groundwater would have been recirculated, which is necessary to explain the apparent multiple discharges of at least some aquifers [9].

Sulfur dioxide has been suggested as a possible greenhouse gas on early Mars [10,11,12]. Mars appears to be a sulfur-rich planet [13,14], and the SO_2/CO_2 ratio found in many Shergottite samples seems to imply that sulfate may have dominated over carbonate in the shock-melted materials [15]. In addition, Wanke et al. [16] have recently suggested that liquid SO_2, or a mixture of liquid SO_2 and CO_2, may be alternatives to liquid H_2O in carving the valley networks.

The primary objection to SO_2 as a major gas in the early martian atmosphere is its relatively short atmospheric lifetime. In the presence of odd hydrogen species, SO_2 is fairly quickly oxidized to SO_3 (as an intermediate step to forming sulfate aerosols). In Earth's stratosphere the lifetime of SO_2 has been estimated to be around 3–4 months, while in a volcanically perturbed martian atmosphere (under present-day conditions), SO_2 may have a lifetime as long as 6 (Earth) years [17]. Recent measurements of the massive SO_2 clouds from the Mt. Pinatubo eruptions have implied that the atmospheric lifetime of SO_2 on Earth may be longer than previously estimated [18].

Previous studies looked at the effect of atmospheric SO_2 on global climate, based on estimates by Greeley [19] of volcanic material erupted during each martian epoch [12]. It was shown that, under ideal conditions, SO_2 could have potentially raised the mean global surface temperature by about 10 K.

In light of recent revisions of magma generation on Mars during each martian epoch [20], and the suggestions by Wanke et al. [16] that the role of liquid SO_2 should be more carefully explored, we have recalculated the potential greenhouse warming by atmospheric SO_2 on Mars, with an emphasis on more localized effects. In the vicinity of an active eruption, the concentration of atmospheric SO_2 will be higher than if it is assumed that the erupted SO_2 is instantaneously globally distributed. The local steady-state concentration of SO_2 is a function of the rate at which it is released, its atmospheric lifetime, and the rate at which local winds act to disperse the SO_2. We have made estimates of eruption rates, length of eruption, and dispersion rates of volcanically released SO_2, for a variety of atmospheric conditions and atmospheric lifetimes of SO_2 to explore the maximum regional climatic effect of SO_2.

References: [1] Kasting J. F. (1991) *Icarus, 94*, 1–13. [2] Newman M. J. and Rood R. T. (1977) *Science, 198*, 1035–1037. [3] Gough D. O. (1981) *Solar Phys., 74*, 21–34.

(to which all ratios are referenced), which replicates quite well the martian composition inferred from SNC meteorite EETA 79001.

No further losses by hydrodynamic escape occur for the next ~80 m.y., until the atmospheric H_2 supply is replenished by an episode of planetary outgassing that also transports noble gases, CO_2 and N_2 gases from interior planetary reservoirs into the atmosphere. Degassed solar-composition Kr, Ar, and Ne mix with atmospheric residues surviving from EUV-1, altering abundances and isotopic compositions (Fig. 1). (As in the original models [5], little if any solar-composition Xe can be outgassed, and so their most crucial assumption also applies here: that Xe tends to partition preferentially into solid phases under conditions of high pressure deep in planetary interiors). For Kr, this mixing generates a composition close to EETA 79001 ratios (Fig. 1). With a new atmospheric H_2 supply (~20 bars), escape resumes, now driven by a diminished solar EUV flux too weak to enable Kr (or Xe) loss. Parameters of this EUV-2 episode, chosen to fractionate residual $^{36}Ar/^{38}Ar$ to the remarkably low SNC value of 4.1, lead to overfractionation of $^{20}Ne/^{22}Ne$ as seen in Fig. 1. However post-escape addition of solar wind (SW) noble gases to the planet could have elevated a lower $^{20}Ne/^{22}Ne$ ratio to its present value without sensibly affecting heavier species. The required Ne contribution is roughly equal to the SW-Ne content of ~20 g/cm^2 of interplanetary dust particles deposited on Mars; the implied IDP flux to the planet over 3–4 b.y. is not far above current estimates [5].

Atmospheric Erosion: This model, given its assumptions, reproduces martian noble gas abundances and the EETA 79001 isotopic compositions within error. However, Mars, small and low-g, is particularly vulnerable to loss of atmospheric gases by impact ejection [9,10], particularly prior to ~3.5–3.8 b.y. ago during epochs of high and energetic projectile fluxes in the final stages of planetary accretion and the "late heavy bombardment" registered on ancient lunar surfaces. Zahnle [10] concludes that the planet could well have been completely denuded of atmophiles prior to ~100 m.y., with the present atmosphere deriving from a small volatile remnant sequestered in the megaregolith and later degassed. This view is not inconsistent with models of isotopic evolution by hydrodynamic escape. The initial Xe content of the primary martian atmosphere in the model above is lower by a factor of ~5000 than would have been supplied to the planet by accretion of the same g/g-planet abundance of "solar-like" icy planetesimals as Venus, and by a 40% mass component resembling CI meteorites [8] in volatile loading. Losses prior to initiation of escape at ≥100 m.y. were evidently enormous, and both the water supplying atmospheric hydrogen, and the other primary atmospheric constituents, could have degassed at this time from regolith sites sheltered from earlier ejection by impact. Atmospheric erosion *during* the hydrodynamic escape epoch, which extends over the following ~135 m.y., can be readily accommodated in the model via the Melosh-Vickery [9] analytic erosion formalism and heavy bombardment projectile flux distribution for Mars. Since the extents of erosive atmospheric losses in periods of low H_2 pressure—during the ~80-m.y. hiatus prior to outgassing, and following the end of hydrodynamic escape at ~235 m.y.—depend critically on the pressures of other species (here, in particular, of CO_2 from the abundant CI component), they are best discussed in the context of a specific model for origin of martian CO_2 and N_2.

Carbon Dioxide and Nitrogen on Mars: Abundances of CO_2 and N_2 in the primary atmosphere are assessed from Xe abundances and the known (or inferred) CO_2/Xe and N_2/Xe ratios in the CI and Venus-like ("solar") components. The CI source dominates these inventories by a wide margin. However, they are small enough that after depletion by both EUV-1 and EUV-2, primary inventories fail to account for contemporary martian N_2 and only marginally reproduce the present atmospheric CO_2 inventory even without impact erosion. Thus, in the particular model outlined here, I assume that a buried CI volatile component was degassed at ~205 m.y., along with solar-composition gases from the deep core reservoir, in amount sufficient to leave the planet with ~5× its present N_2 inventory—thus providing a minimal reservoir for subsequent N_2 depletion and elevation of $\delta^{15}N$ by nonthermal escape—*after* EUV-2 and later erosive losses. The CO_2 in this degassed CI component could have suffered one of two extreme fates. If all released to the atmosphere at ~205 m.y. along with the N_2 and noble gases, the severely fractionated $\delta^{13}C$ of the residual CO_2 surviving EUV-2 requires mixing with 8 bars of CI-composition CO_2, at some time after the end of escape, in order to match contemporary martian $\delta^{13}C$ (taken to be ≈0‰, but uncertainties are large [11]). Alternatively one could propose that outgassing of chemically active CO_2 was delayed for ≥30 m.y., until some time after the termination of EUV-2; in this case 1.5 bars of unfractionated CO_2 could later have entered the atmosphere. Both scenarios are climatologically interesting, in the context of an early greenhouse on Mars, if these relatively large amounts of atmospheric CO_2 were not sequestered in carbonate rock or otherwise removed for an extended period, say until ~3.8 b.y. ago or thereabouts.

With any particular choice for the degassing and atmospheric residence histories of carbon dioxide (there are of course many possibilities other than these two), specification of the surviving N_2 inventory after EUV and erosive losses, and the constraint that post-EUV and post-erosive noble gas abundances must match contemporary atmospheric inventories, depletions by impact ejection during each stage of atmospheric evolution may be calculated in a straightforward way by iteration of the hydrodynamic escape and Melosh-Vickery analytic equations. For the extreme, perhaps unlikely, case of high-pressure CO_2 survival until ~3.8 b.y. ago, overall erosive depletions of noble gases from ~100 m.y. to the present are about a factor of 8, and so initial abundances in the primary atmosphere are higher than those shown in Fig. 1 by this factor, and losses in earlier epochs correspondingly smaller.

References: [1] Reviewed by Donahue T. M. and Pollack J. B. (1983) in *Venus*, pp. 1003–1036, Univ. Ariz., Tucson. [2] Hunten D. M. et al. (1987) *Icarus, 69*, 532–549. [3] Zahnle K. J. and Kasting J. F. (1986) *Icarus, 68*, 462–480. [4] Zahnle K. J. et al. (1990) *Icarus, 84*, 502–527. [5] Pepin R. O. (1991) *Icarus, 92*, 2–79. [6] Pepin R. O. (1992) *LPSC XXIII*, pp. 1053–1054. [7] Zahnle K. J. et al. (1990) *GCA, 54*, 2577–2586. [8] Dreibus G. and Wanke H. (1987) *Icarus, 71*, 225–240. [9] Melosh H. J. and Vickery A. M. (1989) *Nature, 338*, 487–489. [10] Zahnle K. J. (1992) *JGR*, submitted. [11] Jakosky B. M. (1991) *Icarus, 94*, 14–31.

[4] Graedel T. E. et al. (1991) *GRL, 18*, 1881–1884. [5] Sagan C. and Mullen G. (1972) *Science, 177*, 52–56. [6] Kasting J. F. et al. (1991) In *Workshop on The Martian Surface and Atmosphere Through Time*, pp. 71–72, LPI, Houston. [7] Kuhn W. R. and Atreya S. K. (1979) *Icarus, 37*, 207–213. [8] Heinrich M. N. et al. (1991) In *Workshop on The Martian Surface and Atmosphere Through Time*, p. 56, LPI, Houston. [9] Goldspiel J. M. and Squyres S. W. (1991) *Icarus, 89*, 392–410. [10] Postawko S. E. and Kuhn W. R. (1986) *JGR, 91*, D431–D438. [11] Kondratyev K. Y. et al. (1986) *Earth, Moon, and Planets, 35*, 13–18. [12] Postawko S. E. et al. (1987) In *LPI Tech. Rpt. 88-05*, p. 103–104. [13] Clark B. C. and Baird A. K. (1979) *JGR, 84*, 8395–8403. [14] Clark B. C. et al. (1982) *JGR, 87*, 10059–10067. [15] Gooding J. L. et al. (1988) *GCA, 52*, 909–915. [16] Wanke H. et al. (1992) In *LPSC XXIII*, pp. 1489–1490. [17] Settle M. (1979) *JGR, 84*, 8343–8354. [18] Bluth G. J. S. et al. (1992) *GRL, 19*, 151–154. [19] Greeley R. (1987) *Science, 236*, 1653–1654. [20] Greeley R. and Schneid B. D. (1991) *Science, 254*, 996–998.

N92-28505

The Thermal Structure, Dust Loading, and Meridional Transport in the Martian Atmosphere During Late Southern Summer.

M. Santee[1] and D. Crisp[2], [1]170-25 Caltech, Pasadena CA 91125, USA, [2]Jet Propulsion Laboratory, Pasadena CA 91109, USA.

Atmospheric transport may be a crucial element in the seasonal cycles of carbon dioxide, dust, and water on Mars, but the extent of its contribution remains uncertain. The Viking Landers measured surface winds at their respective landing sites [1], and recent ground-based observations constrain the flow in the middle atmosphere (40–70 km) [2], but there have been no direct measurements of the winds in the intervening regions. However, the atmospheric circulation can be calculated diagnostically from the observed atmospheric temperature distribution.

We have derived a comprehensive picture of the thermal structure and dust loading of the martian atmosphere in a relatively clear period during late southern summer [3]. Using a new technique for the simultaneous retrieval of atmospheric temperatures and airborne dust abundances, we examined a subset of the Mariner 9 infrared interferometer spectrometer (IRIS) thermal emission spectra spanning L_s = 343°–348°. Global maps of temperature and dust optical depth as functions of latitude (±90°), altitude (~0–60 km), and Mars local time of day were constructed from the profiles from individual spectra. One of the principal conclusions from this work is that both dayside and nightside atmospheric temperatures at altitudes above about 40 km are warmer over the winter (north) polar regions than over the equator or the summer (south) polar regions. These anomalous temperatures are consistent with ground-based observations of polar warming at higher altitudes (50–85 km) [4,5], and they indicate that the atmosphere is not in radiative equilibrium.

Zonal-mean zonal winds are derived from the observed meridional gradients of the zonally averaged temperatures assuming geostrophy and zero surface zonal wind. They are shown in Fig. 1. The intense eastward jets (with velocities exceeding 120 m/s) correspond to regions of strong horizontal temperature gradients. Similar calculations have been reported previously [6,7], but they were not global in coverage.

Both the zonal-mean meridional circulation and large-scale waves contribute to the north-south atmospheric transport. The net effect of these processes can be approximated by the diabatic circulation, which is that circulation needed to maintain the observed temperature distribution (warm winter pole, cool tropics) in the presence of the radiative drive [8]. A radiative-convective-equilibrium model [9] that accounts for absorption, emission, and multiple scattering by particles and non-grey gases has been used to compute the solar heating and thermal cooling rates from diurnal averages of the retrieved temperature and dust distributions. At pressures below 2.0 mbar, net radiative heating rates in the equatorial region and net radiative cooling rates in the polar regions exceed 6 K/day. We implemented a stream-function model that uses the net radiative heating rates to solve for the meridional and vertical components of the diabatic circulation simultaneously. The diabatic meridional velocity is shown in

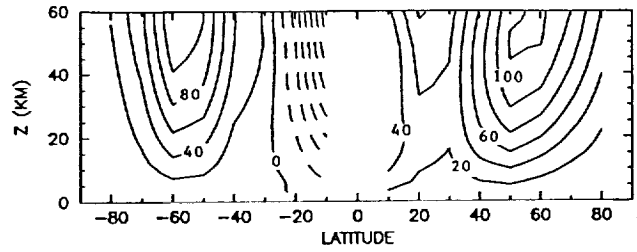

Fig. 1. Geostrophic zonal velocity. Positive eastward, interval = 20 m/s, negative contours dashed.

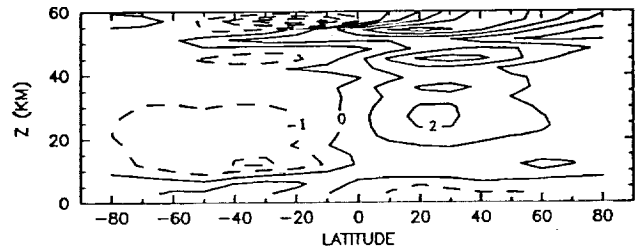

Fig. 2. Diabatic meridonial velocity. Positive northward, interval = 1 m/s, negative contours dashed.

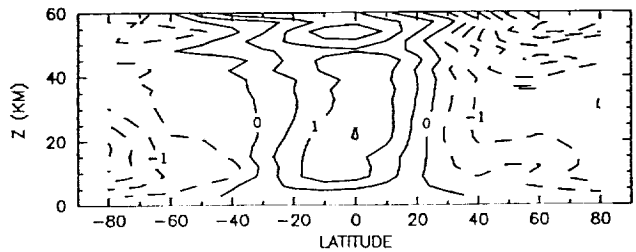

Fig. 3. Diabatic vertical velocity. Positive upward, interval = 0.5 cm/s, negative contours dashed.

Fig. 2, the diabatic vertical velocity in Fig. 3. We find upwelling over the equator (~1.5 cm/s), poleward motion in both hemispheres (~2 m/s), and subsidence over the poles (1–2 cm/s). This is qualitatively similar to the terrestrial equinoctial circulation, and might provide a mechanism for transporting dust and water ice from low latitudes into the polar regions.

References: [1] Hess S. et al. (1977) *JGR, 82*, 4559–4574. [2] Lellouch E. et al. (1991) *Astrophys. J.*, 383, 401–406. [3] Santee M. and Crisp D. (1992) *JGR*, submitted. [4] Deming D. et al. (1986) *Icarus, 66*, 366–379. [5] Rothermel H. et al. (1988) *Astron. Astrophys., 196*, 296–300. [6] Conrath B. (1981) *Icarus, 48*, 246–255. [7] Leovy C. (1982) *Adv. Space Res., 2*, 19–44. [8] Dunkerton T. (1978) *J. Atmos. Sci., 35*, 2325–2333. [9] Crisp D. (1990) *JGR, 95*, 14577–14588.

N92-28506

Volcanic Recycling of Carbonate Deposits on Mars. M. W. Schaefer, Astronomy Department, Universtiy of Maryland, College Park, and Geodynamics Branch, NASA Goddard Space Flight Center, Greenbelt MD 20771, USA.

One question of great interest to those who study the evolution of the martian atmosphere is: if there was an early, dense atmosphere that was removed, is there any mechanism that could restore it? In the case of an atmosphere removed largely by the formation of carbonates [1,2,3], the only obvious means of restoring it is by the thermal decomposition of the carbonates.

Volcanic recycling of carbonates was presented by Pollack et al. [1] as a mechanism for the recharge of Mars' atmosphere, thus allowing a longer period of warm, wet climate. They found burial at depth to be an efficient mechanism for the decomposition of carbonates. But, such burial may be difficult to achieve in the absence of plate tectonics. Another means by which carbonate deposits could be heated to high enough temperatures to decompose is by being covered with lava flows.

Decomposition of carbonates under turbulently flowing lava holds great promise as a means of resupplying the atmosphere with CO_2. Huppert and colleagues [4,5] have modeled the emplacement of terrestrial komatiite flows and found that komatiites, even when flowing over previously emplaced and cooled komatiite flows, could melt and erode this rock to a significant depth. Based on this work, I have begun modeling the erosion of martian carbonate deposits under turbulently flowing, komatiitic lava.

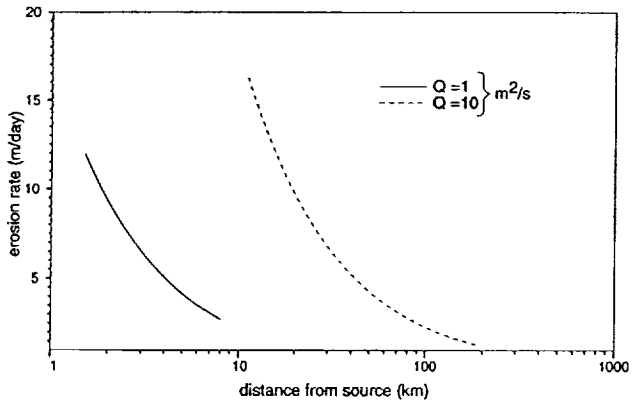

Fig. 1. Carbonate erosion under turbulently flowing komatiitic lava, for different rates of two-dimensional discharge, Q.

Initial results from this modeling indicate that a high-volume lava flow, emerging at a temperature of, say, 1600°, is capable of eroding several meters of carbonate deposits per day (see figure). If such a flow is active for a hundred days, several hundreds of meters of carbonate could be decomposed [3]. If this process occurred over a large area, a bar or more of CO_2 could be injected back into the atmosphere over an extremely short period of time.

The implications of such an occurrence are intriguing. For instance, if a relatively late pulse of volcanism (such as is suggested by Frey [6]) were to cause a large flow of lava over carbonate deposits in the northern lowlands, the resulting pulse of CO_2 into the atmosphere could conceivably restore the climate to one in which liquid water could exist on the surface, or ice could flow.

References: [1] Pollack J. B. et al. (1987) *Icarus, 71*, 203. [2] Schaefer M. W. (1990) *JGR, 95*, 14291. [3] Schaefer M. W. (1992) In *LPI Tech. Rpt. 92-02*, p. 130, LPI, Houston. [4] Huppert H. E. et al. (1984) *Nature, 309*, 19. [5] Huppert H. E. and Sparks R. S. J. (1985) *J. Petrol., 26*, 694. [6] Frey H. (1992) *JGR*, in press.

The Young Sun and the Protoplanetary Environment. F. M. Walter, State University of New York at Stony Brook.

The Sun exerts great influence on the planets, not only gravitationally, but through its irradiance. As the Sun has evolved over the past 4.5 billion years, its bolometric luminosity has increased by 70% (the faint young Sun problem). In addition, as the Sun has aged its rotation has slowed, and the efficiency of its convective dynamo has decreased. The young Sun was far more luminous than the present Sun at X-ray and ultraviolet wavelengths, by factors of over 1000. This ionizing flux is important for studies of the evolution of planetary atmospheres. I shall discuss the likely radiation history of the Sun, based on observations of solar-mass stars in young clusters and associations.

In addition, observations of young stars give clues to when, and how, planets may have formed. I shall discuss the latest searches for evidence of circumstellar disks surrounding the naked T Tauri stars. Our conclusion is still that the inner dust disks of most stars disappear within 100,000 years. I shall speculate about the gaseous component of the disks, and implications for planet formation.

The Role of SO_2 on Mars and on the Primordial Oxygen Isotope Composition of Water on Earth and Mars. H. Wänke, G. Dreibus, E. Jagoutz, and L. M. Mukhin, Max-Planck-Institut für Chemie, Saarstrasse 23, D-6500 Mainz, Germany.

SNC-meteorites are generally considered to represent igneous rocks from the surface of Mars ejected into space by large impacts. Two of the four known shergottites, i.e., Shergotty and Zagami, have a composition very similar to the Viking soil. Thus, the large concentrations of sulfur (3.5%) and chlorine (0.8%) in the Viking soil [1] seem not to be noticeably accompanied by respective cations. The most likely cations for the sulfates, Mg and Ca, have even higher concentrations in Shergotty

and Zagami as has the Viking soil. This observation speaks for a direct introduction of SO_2 and probably also HCl to the martian regolith via gas-solid reactions. The total amount of carbonates in the Martian soil is thought to be less than 2%. Water, SO_2, CO_2, as well as HCl are volcanic exhalation gases, dominantly produced between 4.5 and 3.5 b.y. ago. The presence of SO_2, which will, at least partly, quickly be transformed to SO_3, together with even minimal amounts of water, makes carbonate formation only possible if CO_2 is in excess of SO_2.

To estimate the water content of the martian mantle, Dreibus and Wänke [2] used data on the water content of Shergotty of 180 ppm measured by Yang and Epstein [3]. Shergotty is enriched in La by a factor of 5 relative to the martian mantle. Assuming a similar enrichment for H_2O, a mantle concentration of 180:5=36 ppm was found. This is exactly the value obtained earlier by Dreibus and Wänke [4], comparing the solubility of H_2O and HCl in silicate melts and using the abundance of chlorine in the martian mantle as deduced from SNC meteorites. The exact match is, of course, purely fortuitous considering the uncertainties.

Over the years, the dry martian mantle as proposed by Dreibus and Wänke [2] has been questioned in light of water-rich inclusions observed in SNC meteorites [5]. However, it was not known if the host phases of these inclusions have crystallized from mantle-derived magmas or represent material from a water-rich martian crust taken up by intrusions and overplating of mantle derived magmas. The contradictory evidence of a dry martian mantle as indicated by the low water content of SNC meteorites and the erosional martian surface features, which seem to require large amounts of water, has recently been discussed by Carr and Wänke [6].

The value of 180 ppm H_2O for Shergotty could be considered to be too low as the sample was preheated to 350°C to remove water of terrestrial origin. In this respect highly interesting results were recently obtained by Karlsson et al. [7], who extracted 640 ppm H_2O from Shergotty without preheating and 260 ppm above 350°C. However, the oxygen isotopes indicate that for all the SNC meteorites, aside from the presence of terrestrial contamination, a large fraction of the water, although martian, is not derived from the martian mantle, but obviously represents martian surface water with an oxygen isotope composition up to three times further away from the terrestrial isotope fractionation line than the oxygen in the silicates of SNC meteorites. At the high temperatures during magma generation in the martian mantle isotopic equilibration between oxygen of the silicates and of water would certainly have been established. Hence, only a fraction of the water found in SNC meteorites can be mantle derived and the other nonterrestrial part must come from the martian surface. If the oxygen isotopes of the surface component were created by nonlinear isotope fractionation process the total amount of water of this composition must be small.

Of course, it could also be that the water added to Mars during accretion had oxygen isotopes much further away from the terrestrial isotope fractionation line than the oxygen of martian mantle silicates and that isotopic equilibration of these two oxygen reservoirs never took place. Such a scenario has severe consequences for the accretion processes; it is discussed in more detail by Carr and Wänke [8]. Even in the case of the Earth, if it has received most of its present water by a late veneer, it might be that this water, having oxygen isotopes similar or identical to the martian water, was added without isotopic equilibration with the mantle. Later on, subduction and recycling of the oceanic crust might have continuously brought water from the surface into the originally dry mantle and isotopic equilibration with the oxygen of the silicates took place there.

Let us first consider a possible loss of H_2O from the Shergotty magma during ascent and prior to crystallization. In order to do so, we compare the ratios of volatile resp. moderately volatile elements. The H_2O/Cl ratio in C1-chondrites is 105, terrestrial ocean water (H_2O/Cl = 50) is only a factor 2 lower and even MORB samples are with a ratio of 35 not far off. Shergotty contains 108 ppm chlorine [2], together with 180 ppm H_2O we find a H_2O/Cl ratio of 1.7, a value more than an order of magnitude below this ratio in terrestrial basalts. The K/Cl ratio of C1-chondrites is 0.8, while in MORB and other terrestrial basalts this ratio varies between 13 and 26, indicating the large depletion of the volatile element chlorine compared to the moderately volatile element K. The K/Cl ratio of 15 for Shergotty indicates no significant loss of chlorine from the magma if we assume similar K/Cl ratios for Earth and Mars. No loss of chlorine indicates no substantial loss of H_2O as well.

In total, the 36 ppm water in the martian mantle as estimated by Dreibus and Wänke [2] cannot be substantially too low but they might be too high. If we take the 180 ppm H_2O in Shergotty at face value and compare it with the 1330 ppm S and 620 ppm C in Shergotty, it is evident that sulfur and carbon, respectively SO_2 (2660 ppm) and CO_2 (2270 ppm), are the most abundant volatiles in the Shergotty magma. MORBs contain about 2100 ppm H_2O and about similar concentrations of CO_2 and SO_2. Generally the amount of sulfur in basalts is governed by sulfide solubility. The clear evidence for extraction of chalcophile elements from the martian mantle due to segregation of FeS is in line with the high abundance of sulfur in shergottites. This is even more so if we take into account that the solubility of sulfur in mafic melts increases with increasing FeO content [9] and taking into account that the FeO content of shergottites exceeds that of terrestrial basalts by about a factor of 2.

Reflecting the similar abundances of H_2O, CO_2 and SO_2 in terrestrial magmas, these three compounds are also found in about equal abundances in the gases of terrestrial volcanoes. On a planet with a mantle considerably poorer in water than the Earth, but similar or richer in SO_2, it is to be expected SO_2 to dominate the exhalation gases although part of the sulfur might degas in form of H_2S and elemental S.

In order to explain the run-off channels and valley networks present on the ancient, heavily cratered martian terrain, it was suggested that Mars was warmed by the greenhouse effect of a dense CO_2 atmosphere [10,11]. However, recent work by Kasting [12] has shown that this mechanism does not work in the early solar system history when the luminosity of the Sun was about 25–30% lower than today because of the formation of CO_2 clouds. SO_2 is an very efficient greenhouse gas and its importance for heating of the martian atmosphere was pointed out by Postawko and Kuhn [13].

At present the mean surface temperature of Mars at low latitudes is 218 K or –55°C, while on the poles the temperature drops to less than –140°C. Considering the lower solar luminosity 3.5 b.y. ago, the equatorial mean temperature would drop to about 200 K or –73°C or close to the freezing point of SO_2. Thus, without an appreciable greenhouse effect, H_2O should have been a solid at all latitudes, CO_2 a solid or gas depending on latitude, and SO_2 a liquid or solid depending on latitude. On

Earth the CO_2 from erupting lavas amounts to less than 10% of the amount of CO_2 emitted to the atmosphere from fracture zones and diffusive loss through volcano flanks. Under similar conditions on Mars SO_2, CO_2, and H_2O would migrate through the (mega)-regolith towards the surface. Most of the CO_2 will be quickly transferred to the atmosphere, while SO_2 gas would feed solid, respectively liquid SO_2 tables at low depths. Local warming by a volcanic intrusions will liquefy all the stored SO_2 and drive it to the surface as a liquid at temperatures close to the SO_2 triple point (16 mbar and –73°C).

Liquid SO_2 having a density of 1.61 g/cm^3 at its melting point would lead to similar, but due to its higher density, enhanced, erosional features as water. In fact, liquid SO_2 has been suggested to be responsible to form the complexly eroded scarps on Io [14], which are very similar to such features on Mars. Contrary to H_2O, with its density anomaly, solid SO_2 is 15% denser than the liquid. Thus SO_2 rivers and lakes would not form an SO_2 ice cover to reduce evaporation. However, crystallized SO_2-hydrate floating on liquid SO_2 would be an alternative. In the case of short timely separated discharges, greenhouse warming would be limited to periods in the order of years after discharge of SO_2, as the atmospheric lifetime of SO_2 is limited by photochemical oxidation to SO_3 and atmosphere-surface reactions. Nevertheless, the time could be sufficient to melt water ice stored at or near the surface.

We know that Mars contains considerable amounts of FeS [15]. Although today most of the FeS resides in the martian core, a certain fraction has remained in the mantle, from which sulfur-rich magmas were formed. Formation of SO_2 requires a source of oxygen. The martian soil contains about 3.5% S most probably in the form of sulfates. The oxygen required to transform FeS to SO_3, respectively sulfate, may have had an important influence on the oxygen fugacity of the martian surface and might well be the limiting factor for water. As water is the most likely source of oxidation to transform SO_2 released into the atmosphere to SO_3, we have to ask what portion of water once present at the martian surface was used up for this process. In general the processes for the transformation of SO_2 to sulfate demand an exact quantitative analysis [16]. Contact metamorphism or direct infiltration of magma into the regolith containing sulfates would lead to their decomposition and generation of SO_2. In this way one might even visualize recycling of SO_2.

In summary, we like to stress the importance of SO_2 on Mars. In the case that water should have been supplied in sufficient quantities to the martian surface by a late veneer and stored in the near surface layers in form of ice, temporary greenhouse warming by SO_2 after large SO_2 discharges may have been responsible for melting of ice and break-out of water in areas not directly connected to volcanic activity. Aside of water, liquid SO_2 could explain at least some of the erosion features on the martian surface.

References: [1] Clark B. C. et al. (1982) *JGR, 87*, 10059. [2] Dreibus G. and Wänke H. (1989) In *Origin and Evolution of Planetary and Satellite Atmospheres*, pp. 268–288, Univ. Ariz. [3] Yang J. and Epstein S. (1985) *LPSC XVI, Suppl. A*, p. 25; [4] Dreibus G. and Wänke H. (1987) *Icarus, 71*, 225. [5] Johnson M. C. et al. (1991) *GCA, 55*, 349. [6] Carr M. and Wänke H. (1991) *LPSC XXII*, p. 181. [7] Karlsson H. R. et al. (1991) *Meteoritics*, in press. [8] Carr M. and Wänke H. (1992). [9] Haughton D. R. et al. (1974) *Econ. Geol., 69*, 451. [10] Moroz V. I. and Mukhin L. M. (1977) *Cosmic Res., 15*, 769. [11] Pollack J. B. et al. (1987) *Icarus, 71*, 203. [12] Kasting J. F. (1991) *Icarus, 94*, 1. [13] Postawko S. E. and Kuhn W. R. (1986) *JGR, 91*, D431. [14] McCauley J. F. et al. (1979) *Nature, 280*, 736. [15] Wänke H. and Dreibus G. (1988) *Phil. Trans. R. Soc. Lond., A325*, 545. [16] Settle M. (1979) *JGR, 84*, 8343.

N92-28508

Martian Surficial Carbon—Constraints from Isotopic Measurements of Shock-Produced Glass in EET A79001.

I. P. Wright, C. P. Hartmetz, and C. T. Pillinger, Department of Earth Sciences, Open University, Walton Hall, Milton Keynes MK7 6AA, U.K.

The gases trapped in shock-produced glass from the EET A79001 shergottite (one of nine SNC meteorites) appear to represent a sample of the martian atmosphere [1–4]. It is therefore possible to undertake a detailed study of the martian atmosphere using state-of-the-art equipment in laboratories on Earth; thus far, noble gases have been analyzed, in addition to nitrogen and carbon dioxide. The distribution and isotopic compositions of the entrapped noble gases have been interpreted as the result of an early hydrodynamic escape episode on Mars [5,6]. Isotopic measurements of nitrogen in the glass from EET A79001, while serving to substantiate a martian origin for the meteorite, are compromised by the presence of magmatic forms of the element, which act to dilute the true isotopic composition of the atmospheric species. Models of the evolution of the martian atmosphere based solely on nitrogen data are, therefore, more satisfactorily derived using measurements obtained from Viking [7,8].

The bulk of the martian atmosphere is CO_2—clearly it is desirable to understand the evolution of this major atmospheric constituent. To this end it is noteworthy that Viking data indicate no large fractionation effects in either $^{12}C/^{13}C$ or $^{16}O/^{18}O$, implying that CO_2 is in isotopic equilibrium with the surface of Mars. This is readily understood since CO_2 takes part in the cycling of volatiles through the polar cap-regolith-atmosphere system. To evaluate in more detail the nature of volatile cycling on Mars, the carbon isotopic composition of CO_2 trapped in the glass from EET A79001 has been determined [4]. It is found that there is a small, but significant, enrichment of ^{13}C in the trapped CO_2, compared to martian crustal carbon; this has been interpreted as evidence for an atmospheric loss process [9].

An additional control on the understanding of CO_2 cycling on Mars comes from an evaluation of isotopic compositions of the carbonate minerals in SNC meteorites. It has been shown that there is a sympathetic relationship between $\delta^{13}C$ and $\delta^{18}O$ in carbonates from different SNC meteorites [10]. Although attempts have been made to interpret this as a reflection of variable formation conditions (temperature, H_2O/CO_2 ratio), it is clear that a simple-minded approach cannot satisfy the isotopic constraints. It is therefore possible that the variation in $\delta^{13}C$ with $\delta^{18}O$ represents mixing of two different sorts of carbonate minerals. EET A79001 is known to contain two varieties of carbonate: anhedral crystals of 20-μm size enclosed in shock-produced glass, plus more extensive deposits (known as white druse) found in the interior of the meteorite as an infilling of void spaces [11]. Attempts to distinguish between the carbonates on the basis of isotopic measurements have thus far proved inconclusive [12,13]. However, the $\delta^{13}C$ value of carbonates in EET A79001, made by different laboratories, spans a range of +3 to +10‰, while $\delta^{18}O$

^{129}Xe, daughter of the extinct radionuclide ^{129}I (half-life 17 Myr). In impact erosion the first two become constraints on the composition, mass distribution, and orbital elements of the impactors. The third requires that Mars lost its nonradiogenic Xe early, probably before it was 100 Myr old [3]. Impact erosion can explain Mars by any of three stories. (i) Mars is unlikely. In a sort of planetary brinkmanship, impact erosion almost removed the entire atmosphere but was arrested just in time. (ii) Martian noble gases are cometary and cometary Xe is as isotopically mass fractionated as martian and terrestrial Xe [4]. This is most easily accomplished if a relatively thick geochemically controlled CO_2 atmosphere protected trace atmophiles against escape. (iii) Mars was indeed stripped of its early atmosphere but a small remnant was safely stored in the regolith, later released as a byproduct of water mobilization.

References: [1] Anders E. and Owen T. (1977) *Science, 198*, 453–465. [2] Kahn R. (1985) *Icarus, 62*, 175–190. [3] Musselwhite D. S. et al. (1991) *Nature, 352*, 697–699. [4] Owen T. et al. (1991) In *Comets in the Post Halley Era* (R. Newburn, M. Neugebauer, and J. Rahe, eds), pp. 429–438.

Spectral Identification of Chemisorbed CO_2 and Application to Mars Analog Materials. A. P. Zent[1] and T. L. Roush[2], [1]SETI Institute and NASA Ames Research Center, Moffett Field CA 94035, USA, [2]San Francisco State University, San Francisco CA 94132 and NASA Ames Research Center, Moffett Field CA 94035, USA.

Introduction: The goal of this work is to identify the spectral signature of chemisorbed CO_2, to test the efficacy of carbonate formation on Mars-analog materials via CO_2 chemisorption, and to identify the surface-chemical characteristics of good chemisorbents, with the intent of assessing the possible geochemical importance of CO_2 chemisorption as a quasipermanent CO_2 sink in the martian environment.

Our approach is to search for infrared spectral bands that result from chemisorption of CO_2 molecules onto chemical reagents and Mars-analog materials, and to identify the salient differences in adsorbents that favor strong, permanent CO_2 chemisorption.

The total amount of CO_2 in the early martian atmosphere, and consequent surface temperatures, are unknown [1]. A CO_2 greenhouse may not have been an adequate mechanism under any circumstances [2]; however, if it were, then most of that CO_2 must still be in the near-surface environment; no escape mechanism that could remove it after the decline of channeling has been identified. The only plausible reservoir is carbonate, and there are various remote sensing techniques that can be used to search for it [3]. We are investigating CO_2 chemisorption as a permanent CO_2 sink, and to aid in interpretation of remotely sensed IR spectra of Mars.

A common effect reported in CO_2 adsorption studies is the formation of a layer of carbonate or bicarbonate anions on adsorbents that have OH^- groups available on their surfaces. Inorganic hydroxyls occur on phyllosilicates, amorphous silicates, metal oxides and hydroxides; it is the most abundant and reactive surface functional group on the surfaces of terrestrial silicates [5]. The process responsible for the reaction is *chemisorption*. Chemisorption is distinguished from physical adsorption in that there is a transfer of electrons between species, and the formation of a chemical bond. The heat of chemisorption is typically of the same order as heats of chemical reaction (i.e., a few hundred to a few thousand kJ/mole), as opposed to heats of physical adsorption (a few kJ per mole). Chemisorption is an activated process that is promoted by an increase in temperature—quite the opposite of physical adsorption. Chemisorption is not reversible in the sense that physical adsorption is.

Experiment: We selected CaO and $Ca(OH)_2$ as reference materials because they have been reported in the literature to form carbonate and bicarbonate ions by CO_2 chemisorption within minutes [5]. As Mars analog materials, we used montmorillonite and a palagonite collected from the summit of Mauna Kea.

Samples were prepared by sealing powdered samples in serum vials and purging the head space with CO_2 at 10^5 Pa, at a flow rate of 4 ml min^{-1} for approximately 24 hours. Controls were sealed at the same time as the samples but not exposed to CO_2 Controls and samples were simultaneously warmed slightly to about 310 K to maximize chemisorption and minimize physical adsorption. These conditions may be representative of a warm, wet climate on early Mars, and are conducive to CO_2 chemisorption. After 24 hours, the powders were removed from the serum vials and 0.2 mg were mixed with approximately 200 mg of KBr and pressed into pellets. The pellets were placed in the spectrometer, which was purged with dry N_2. N_2 purge throughout data acquisition further reduces the abundance of physical adsorbates. Transmission spectra were acquired from 400 to 4000 cm^{-1} with a resolution of 1 cm^{-1}. Differences in thickness and concentration were corrected by calculating the mass extinction coefficient via:

$$\varepsilon = \frac{-\log_{10}(I/I_o)}{Ct}$$

where ε is the mass extinction coefficient, C is the concentration of powder in the pellets, t is the pellet thickness and I/I_o is the transmission. After continuum removal, extinction peaks were plotted for all powders.

CaO and $Ca(OH)_2$: There were pronounced effects on the $Ca(OH)_2$ and CaO spectra caused by exposure to CO_2 (Figure 1). Bands at 875, 1034, and 1070 cm^{-1} showed a strong increase in extinction. In addition, strong fundamental bands at 1425 to 1480 cm^{-1} increased by several tens of percent. The locations of these bands correspond to reported bands in the spectra of various forms of the CO_3^{2-} anion reported in the literature [6,7], and we ascribe their growth in this experiment to the chemisorption of gaseous CO_2. By examining these species, we have demonstrated that our technique is sensitive to carbonate and bicarbonate formation in powdered samples, and identified spectral regions that are diagnostic of the reaction under consideration.

varies by only 1‰ [14–16]. These results do not follow the normal variation in $\delta^{13}C$ with $\delta^{18}O$, suggesting that EET A79001 may contain *additional* carbonate minerals (of a different origin?). Such a hypothesis is supported by ^{14}C measurements, which indicate that the white druse in EET A79001 may have formed as a result of Antarctic weathering on Earth [14]. Additionally, recent measurements of the oxygen isotopic composition of water liberated from SNC meteorites [17] show EET A79001 to be 10–20‰ lower in $\delta^{18}O$ than other samples, implying a terrestrial (Antarctic) input of some description. If white druse carbonates also formed on Earth it may be anticipated that the oxygen isotopic compositions of these minerals might be somewhat lighter than those in other SNC meteorites. However, it should be noted that the $\delta^{18}O$ of white druse in EET A79001 is only ca. 2–3‰ lighter than the non-Antarctic sample, Nakhla. Thus, the origin of the white druse is still not easily explained.

In a once simple picture, it was proposed that martian carbonates and atmospheric CO_2 were genetically related since both species were considered to be enriched in ^{13}C to about the same extent (i.e., $\delta^{13}C$ ca. +15‰). However, as a unique carbon isotopic composition for all the carbonates in SNC meteorites can no longer be specified, the exact relationship between CO_2 and carbonates is unclear. In order to try and clarify the situation, we have re-analysed the carbon contained in the shock-produced glass in EET A79001 using stepped combustion; carbon isotopic measurements have been made using a new mass spectrometer [18]. The total carbon yield for the experiment is 58.2 ppm, with a bulk $\delta^{13}C$ of–17.8‰ (which compares with 48.0 ppm and $\delta^{13}C$ of –20.7‰ for the earlier analysis). The agreement between the two analyses is considered good, when account is taken of the variable $\delta^{13}C$ values of the different components in SNC meteorites, and the possibilities of sample heterogeneity. In addition, the release profiles of the two experiments are qualitatively similar; both exhibit a large release of carbon below 400°C (37.1 and 14.9 ppm C) predominantly from terrestrial organic contamination. In the new analysis there is a release of carbon from carbonate at 475–630°C, which has an elevated $\delta^{13}C$ (up to +4.9‰). It is considered likely that this carbonate mineral is associated with the glass, since white druse deposits are visually absent from this sample. Interestingly the carbon isotopic composition of the glass-related carbonates is not substantially different to that of white druse, which gave a maximum $\delta^{13}C$ of +8.9‰ during stepped combustion [15].

At the highest temperatures of extraction, trapped martian atmospheric CO_2 is released. For this component, $\delta^{13}C$ rises to +27‰ (compared to +15‰ previously). Because of the possibilities that ^{13}C-rich atmospheric CO_2 is released along with ^{13}C-depleted crustal carbon, the highest $\delta^{13}C$ value measured represents a lower limit to the true isotopic composition of the atmospheric species. Thus, the new $\delta^{13}C$ determination is considered to best represent martian atmospheric CO_2. Based on a $\delta^{13}C$ of +27‰, and a release temperature of 1000–1200°C, the new analysis shows the glass to contain 2.4 ppm C as CO_2, compared to 5.5 ppm C previously. Thus, it would seem that trapped CO_2 is distributed rather unevenly throughout the glass.

References: [1] Bogard D. D. and Johnson P. (1983) *Science, 221*, 651–654. [2] Becker R. H. and Pepin R. O. (1984) *EPSL, 69*, 225–242. [3] Wiens R. C. et al. (1986) *EPSL, 77*, 149–158. (4) Carr R. H. et al. (1985) *Nature, 314*, 248–250. [5] Hunten D. M. et al. (1987) *Icarus, 69*, 532–549. [6] Pepin R. O. (1991) *Icarus, 92*, 2–79. [7] Owen T. et al. (1977) *JGR, 82*, 4635–4639. [8] McElroy M. B. et al. (1976) *Science, 194*, 70–72. [9] Wright I. P. et al. (1990) *JGR, 95*, 14789–14794. [10] Wright I. P. et al. (1992) *GCA, 56*, 817–826. [11] Gooding J. L. et al. (1988) *GCA, 52*, 909–915. [12] Hartmetz C. P. et al. (1991) *Workshop on MSATT*, pp. 54–55. [13] Wright I. P. et al. (1992) *JGR*, submitted. [14] Jull A. J. T. et al. (1992) *LPSC XXIII*, pp. 641–642. [15] Wright I. P. et al. (1988) *GCA, 52*, 917–924. [16] Clayton R. N. et al. (1988) *GCA, 52*, 925–927. [17] Karlsson H. R. et al. (1992) *Science, 255*, 1409–1411. [18] Prosser S. J. et al. (1990) *Chem. Geol., 83*, 71–88.

N92-28509

How Mars Lost Its Atmosphere. Kevin Zahnle, Mail Stop 245-3, NASA Ames Research Center, Moffett Field CA 94035, USA.

Mars is a small planet with a thin atmosphere. That Mars is small has been known for centuries, and we have gotten used to it; but its thin atmosphere has been called "one of the great disappointments of the space age" [1], and we have not gotten used to this. The apparent dearth of volatiles is not confined to one or two key elements, but may well apply to all plausible atmospheric constituents. It is surest for the noble gases, for which alternative reservoirs larger than the atmosphere are unlikely. It is less certain for water or CO_2, which can be hidden in surface and subsurface reservoirs.

There is a widespread suspicion that Mars's thin atmosphere is in some way attributable to the planet's size. Three more or less complementary hypotheses have been suggested. The current favorite is that Mars, being small, cooled relatively quickly, and long ago ceased to recycle volatiles effectively. Weathering reactions of water, CO_2, and rock would then have progressively and irreversibly consumed the atmosphere [2]. This modern incarnation of Lowell's "dying planet" applies to CO_2 and water in particular; it is more problematic for nitrogen, and it is very hard to see how it could apply to the noble gases.

Another possibility is that the atmosphere was never degassed or outgassed in the first place. Although inefficient outgassing of modern Mars is a reasonable hypothesis, and fully consistent with the great antiquity of its few volcanos and the low absolute abundance of ^{40}Ar compared to Earth, inefficient outgassing of ancient Mars is less appealing, and is contradicted by the relatively high abundance of ^{129}Xe in the martian atmosphere.

I prefer escape. Hydrodynamic escape (vigorous thermal escape) and impact erosion (expulsion of atmosphere by impacts) are two processes that should have been operative early. Although in principle hydrodynamic escape could have shrunk Mars's atmosphere a hundredfold while leaving the composition of the remnant atmosphere nearly unaltered, very high escape fluxes are required. The implicated escape mechanism must have been efficient, nearly non-fractionating, and vastly more potent for Mars than for Earth or Venus. Impact erosion is an appealing candidate.

Noble gases are the obvious first test. Noble gases are the most volatile elements and so are the most likely to have been affected by impact erosion and the easiest to address quantitatively. Xenon in particular imposes three constraints on how Mars lost its atmosphere: (i) the very low abundance of nonradiogenic Xe compared to Earth, Venus, and likely meteoritic sources; (ii) its nonradiogenic isotopes distinct from likely meteoritic sources; and (iii) the relatively high absolute abundance of radiogenic

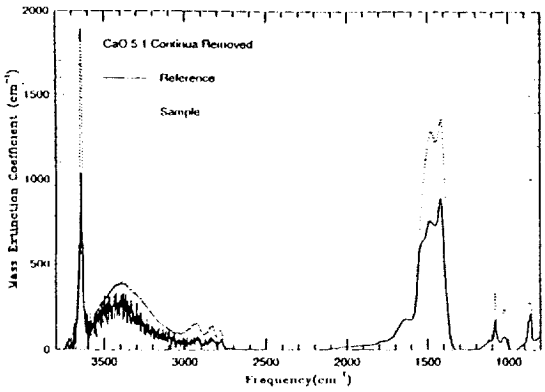

Fig. 1. Mass extinction coefficients for CaO reference and sample.

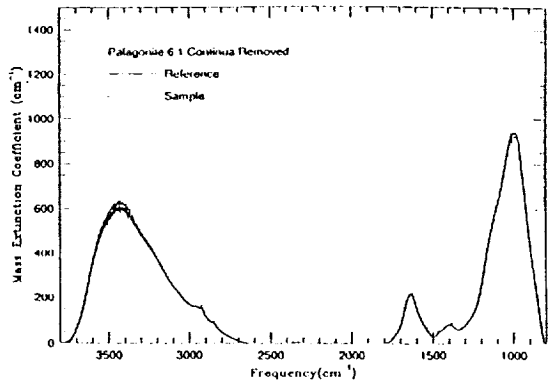

Fig. 2. Mass extinction coefficients for palagonite reference and sample.

Montmorillonite and Palagonite: The depth of the silicate fundamental in both of these materials renders the spectral region from 800 to 1200 cm^{-1} unavailable for testing the chemisorption process. However, the region of the strongest absorption, between 1400 and 1500 cm^{-1}, is largely free of strong absorbers, and a detailed examination of spectral changes in this frequency range was made. The extinction of the samples was greater than that in the reference materials throughout this region at the level of a few percent. However, a detailed examination of the 1400–1500 cm^{-1} range found no increase in apparent band strength above the variation characteristic of the remainder of the spectrum. No positive evidence of the formation of carbonate or bicarbonate anions could be identified in either the montomorillonite or the palagonite (e.g., Figure 2).

Summary: Exposure to 100 kPa of CO_2 for 24 hours at 50°C produced easily detectable amounts of chemisorbed carbonate and possible bicarbonate ion on the surface of CaO and $Ca(OH)_2$. There was no spectral evidence for the formation of either carbonate or bicarbonate upon exposure of montmorillonite and palagonite to the same conditions. Our experiment produced no evidence that significant amounts of CO_2 could be stored irreversibly as carbonate or bicarbonate, nor is there any reason to suspect that infrared studies of the martian regolith must account for chemisorbed CO_2. In future studies we will examine CO_2 chemisorption of 1:1 layer clays, which have more OH^- groups on mineral surfaces, to ascertain whether carbonate or bicarbonate formation proceeds rapidly on those adsorbents.

References: [1] Pollack et al. (1987) *Icarus, 71*, 203–224. [2] Kasting J. (1991) *Icarus, 94*, 1–13. [3] Pollack et al. (1990) *JGR, 95*, 14595–14627. [4] Sposito G. (1984) *Surface Chemistry of Soils*, Oxford. [5] Rosynek M. et al. (1977) *J. Catal., 48*, 417–421. [6] Gadsden J. A. (1975) *Infrared Spectra of Minerals and Related Inorganic Compounds*, Butterworths. [7] White W. B. (1974) In *The Infrared Spectra of Minerals*, Mineral. Soc. Am. Monograph 4.